catalysts

MDPI

Review

Occurrence, Ecotoxicity, and Photocatalytic Remediation of Antiretroviral Drugs in Global Surface Water Matrices

Phephile Ngwenya *, Lehlogonolo S. Tabana, Shepherd M. Tichapondwa and Evans M. N. Chirwa *

Department of Chemical Engineering, Sustainable Environmental and Water Utilisation Processes Division, University of Pretoria, Pretoria 0002, South Africa
* Correspondence: u16252642@tuks.co.za (P.N.); evans.chirwa@up.ac.za (E.M.N.C.)

Abstract: The increasing presence of pharmaceuticals, particularly antiretroviral drugs (ARVs), in wastewater has raised concerns regarding their environmental and health impacts. Photocatalysis, driven by advanced photocatalysts, such as coloured TiO_2, ZnO, and composites with carbon-based materials, has shown promise as an effective method for degrading these pollutants. Despite significant laboratory-scale success, challenges remain in scaling this technology for real-world applications, particularly in terms of photocatalyst stability, the formation of toxic degradation by-products, and economic feasibility. This paper explores the current state of photocatalytic degradation for ARVDs, emphasizing the need for further research into degradation pathways, the development of more efficient and cost-effective photocatalysts, and the integration of photocatalysis into hybrid treatment systems. The future of photocatalysis in wastewater treatment hinges on improving scalability, reactor design, and hybrid systems that combine photocatalysis with traditional treatment methods to ensure comprehensive pollutant removal. Innovations in catalyst design and reactor optimization are essential for advancing photocatalysis as a viable solution for large-scale wastewater treatment.

Keywords: photocatalysis; photocatalyst; TiO_2; ARVDs; degradation efficiency; dosage; wastewater

Academic Editors: Hideyuki Katsumata, Esmeralda Mendoza, Juan Carlos Durán-Álvarez and Socorro Oros-Ruiz

Received: 1 March 2025
Revised: 2 April 2025
Accepted: 10 April 2025
Published: 15 April 2025

Citation: Ngwenya, P.; Tabana, L.S.; Tichapondwa, S.M.; Chirwa, E.M.N. Occurrence, Ecotoxicity, and Photocatalytic Remediation of Antiretroviral Drugs in Global Surface Water Matrices. *Catalysts* **2025**, *15*, 381. https://doi.org/10.3390/catal15040381

1. Introduction

Since the late 1990s, the presence of pharmaceuticals in the environment has been recognized as a substantial concern [1,2]. Among the 4000 active pharmaceutical ingredients (APIs) prescribed globally [3], 771 have been identified within environmental matrices [4]. However, conventional wastewater treatment plants used in numerous countries remain inadequate in their capacity to monitor and eliminate these contaminants, thus, permitting their undetected entry into ecosystems [5]. Antiviral drugs, in particular, are ranked among the most hazardous due to their documented toxicity to aquatic organisms such as algae, daphnids, and fish, as noted by Sanderson et al. [6]. The persistence and bioaccumulation of these pharmaceuticals has raised significant concerns regarding their enduring ecological impacts and the potential for human exposure through contaminated water sources.

Pharmaceutical classes, such as antibiotics like tetracycline, oxytetracycline, and sulfamethoxazole, have been shown to exhibit toxicity in algae, including *Scenedesmus obliquus* and *Chlorella vulgaris*, and possess carcinogenic effects in animals [7]. Similarly, non-steroidal anti-inflammatory drugs (NSAIDs) such as aspirin, ibuprofen, diclofenac, and paracetamol are known not only to impair auditory functions in humans [8] but also, at elevated doses, induce liver damage, toxicity, and potentially fatal outcomes [9]. Russo et al. [10] highlighted that pharmaceuticals of priority should encompass cytotoxic/genotoxic agents, estrogens, and hormones, given their propensity to persist in

aquatic environments and sediments. This persistence enhances the probability of bioaccumulation, particularly among aquatic organisms, with the long-term effects remaining inadequately understood [11]. In light of global initiatives advancing sustainable development practices encompassing wastewater reuse in agriculture [12], soil amendment [13], and material production [14], there is an imperative to eradicate pharmaceutical residues from wastewater effluents to obstruct their perpetual cycling within human and environmental systems.

Conventional wastewater treatment plants (WWTPs) have consistently demonstrated inadequacies in the removal of emerging contaminants, necessitating the implementation of advanced treatment technologies. Common alternatives, as seen in Figure 1, include physical methods (e.g., membrane filtration and adsorption), biological processes (e.g., activated sludge and biofilm systems), and chemical methods (e.g., chlorination and ozonation). However, these approaches often face limitations in completely eliminating persistent and nonbiodegradable organic pollutants. This has driven increasing interest in advanced oxidation processes (AOPs) [15], particularly photocatalysis, which has emerged as an effective and environmentally friendly option. Photocatalysis facilitates the degradation of organic pollutants and nonbiodegradable compounds through the generation of reactive oxidative species [16] and has shown significant efficacy in the elimination of pharmaceuticals [17], pesticides, humic substances, and other hazardous materials from wastewater [18]. Titanium dioxide (TiO_2), esteemed for its non-toxic characteristics, cost-efficiency, and chemical stability, remains the most predominantly utilized photocatalyst [19]. Upon exposure to light, TiO_2 initiates a photoreaction by the excitation of electrons from its valence band to the conduction band, consequently producing reactive holes that promote redox reactions [20]. However, pristine TiO_2 exhibits certain limitations, notably rapid charge recombination and a substantial band gap ranging from 3.0 to 3.2 eV, which confines its activity to ultraviolet (UV) light, merely constituting approximately 5% of the solar spectrum [21].

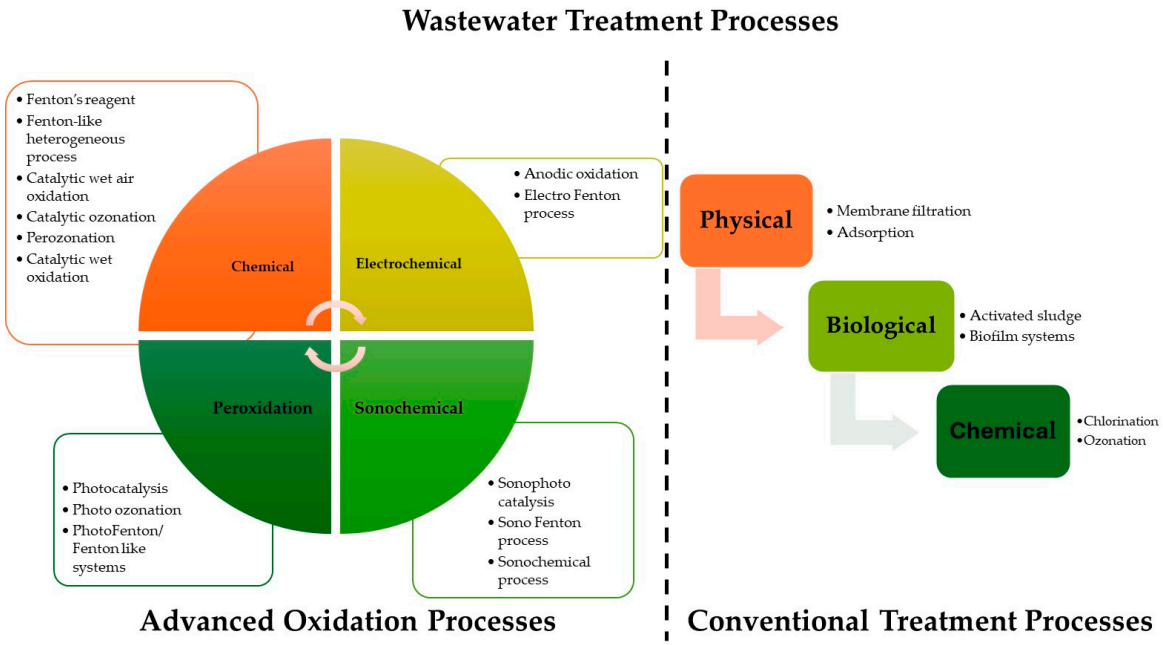

Figure 1. Advanced oxidation processes and conventional treatment processes employed for wastewater treatment.

The discovery of hydrogenated coloured TiO_2 has revolutionized the field of photocatalysis by effectively addressing the performance limitations inherent in TiO_2. Possessing a reduced bandgap of approximately 1.5 eV, coloured TiO_2 demonstrates an enhanced

capability for light absorption within the visible and infrared spectra, thereby considerably augmenting its photocatalytic efficiency [22]. This significant advance has catalyzed a global surge in research efforts, resulting in the development of a variety of synthesis methodologies for the production of hydrogenated or reduced TiO_2, which manifests in different hues, such as yellow, blue, grey, and black, depending on the precursor materials and reaction conditions used [23]. The unique structural attributes and enhanced performance characteristics of coloured TiO_2 present promising opportunities for the removal of APIs from aquatic environments. This review is intended to thoroughly examine the potential of these cutting-edge photocatalysts in addressing pharmaceutical contamination and in furthering sustainable wastewater treatment methodologies.

2. Occurrence of ARVs in Sub-Saharan Africa

Despite the limited literature on the occurrence of antiretroviral drugs (ARVDs) in various waterbodies worldwide, there is a need to postulate the potential effects these APIs may have on the environment. This can be based on measured environmental concentrations (MECs) where data are available. In this study, ARVDs and their metabolites were critically reviewed for their occurrence, ecotoxicity, and remediation. Data were collected from studies conducted in five countries (Finland, Germany, Kenya, South Africa, and Zambia), with 90 sites reported across a total of 12 articles. These studies were used in several reviews on pharmaceuticals, emerging contaminants, and ARVDs in the environment, both in Africa and globally. The aforementioned data were obtained after thoroughly reading through numerous reviews from various scientific journals, primarily from Science Direct and Google Scholar. This process was carried out between June 2023 and May 2024.

Globally, over 30 million people living with HIV/AIDS (PLWHIV) have access to more than 30 ARVDs [24], that have been approved by the Food and Drug Administration (FDA), as shown in Table 1 [25]. These drugs are used in various formulations for the treatment of HIV/AIDS. Consequently, ARVDs are frequently identified among the pharmaceuticals detected in waterbodies in regions where HIV/AIDS is prevalent, as highlighted in Figure 2. Similarly to other pharmaceuticals, ARVDs are not fully absorbed by the human body upon ingestion. Instead, they undergo metabolic transformation, resulting in the formation of active or inactive metabolites. Certain portions of the parent compound and/or its metabolites are subsequently excreted through urine and/or feces [26].

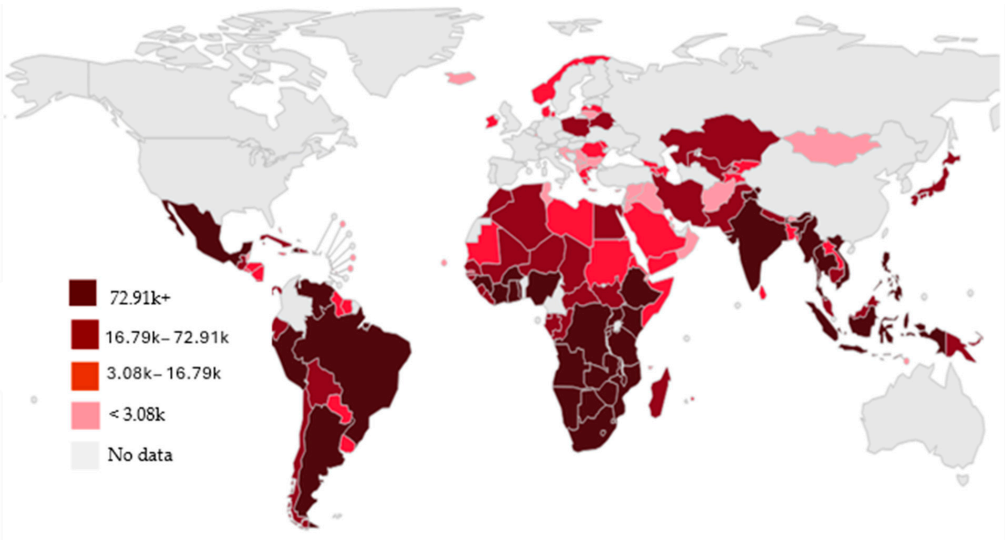

Figure 2. Global statistics on people living with HIV receiving ART (UNAIDS, 2024).

Table 1. Antiretroviral drugs used for the management of HIV/AIDS including their formulation and doses prescribed to patients.

Drug Class	Drug Name			Formulation (mg/Tablet)	Dosage (Tablet. d^{-1})
	Generic	Acronym	Brand		
NRTIs	Abacavir	ABC	Ziagen	300	2
	Emtricitabine	FTC	Emtriva	200	1
	Didanosine	DDI	Videx EC	250	1
	Lamivudine	3TC	Epivir	300	1
	Tenofovir disoproxil Fumarate	TDF	Viread	300	1
	Stavudine	d4T	Zerit	60	1
	Zalcitabine	ddC	Hivid	0.750	3
	Zidovudine	AZT, ZDV	Retrovir	300	1
NNRTIs	Doravirine	DOR	Pifeltro	100	1
	Efavirenz	EFV	Sustiva	600	1
	Etravirine	ETR	Intelence	200	2
	Nevirapine	NVP	Viramune	200	2
	Rilpivirine	RPV	Edurant	25	1
PIs	Atazanavir	ATV	Reyataz	300	1
	Darunavir	DRV	Prezista	800	1
	Fosamprenavir	FPV	Lexiva	700	-
	Ritonavir	RTV	Norvir	100	-
	Saquinavir	SQV	Invirase	200	-
	Tipranavir	TPV	Aptivus	250	-
	Indinavir	IDV	Crixivan	400	-
	Nelfinavir	NFV	Viracept	1250	2
	Lopinavir	LPV	Kaletra	200	1
	Amprenavir	APV	Agenerase	-	-
INIs	Cabotegravir	CAB	Vocabria	30	1
	Dolutegravir	DTG	Tivicay	50	1
	Raltegravir	RAL	Isentress	400	2
E&FIs	Enfuvirtide	T-20	Fuzeon	90	2
	Maraviroc	MVC	Selzentry	300	2
PEs	Cobicistat	COBI, c	Tybost	150	1

Dolutegravir (DTG) and tenofovir (TDF) exhibit excretion rates of 95% and 85%, respectively, with excretion occurring primarily in unchanged form [27]. The occurrence of these compounds in aquatic environments can be attributed to the inefficacies of wastewater treatment plant (WWTP) processes, surface run-off, and the improper disposal of unused ARVDs [28]. The limited efficacy of WWTP processes allows pharmaceuticals, along with their metabolites and transformation products (TPs), to persist in surface waters, as these substances are not effectively removed during treatment [29,30]. Table 1 presents ARVDs used for the management of HIV/AIDS, their classification, generic names, acronyms, brand names, formulations, and doses prescribed to patients.

In many regions of Africa, WWTPs are primarily available in urban areas, leaving a sizeable portion of the population without access to proper wastewater treatment. Consequently, wastewater from peri-urban and rural regions is discharged directly into rivers, thereby contaminating aquatic ecosystems [31,32]. ARVDs present in the environment undergo structural transformations through both biotic and abiotic mechanisms, hence altering the said compounds [33]. South Africa, which has the highest prevalence of PLWHIV and administers the largest antiretroviral therapy (ART) programme servicing approximately 8 million patients, has extensive documentation of these pharmaceuticals in various aquatic environments [34].

There is a growing body of evidence pointing to the presence of ARVDs in surface waters, originating from sources such as manufacturing, human excretion, disposal or discharge, urban discharge, runoff, and ineffectiveness of wastewater treatment processes [35]. WWTP effluent discharge constitutes the principal source of micropollutants in surface water systems, in comparison to alternative sources [36]. Figure 3 illustrates the documented concentrations of ARVDs globally, with South Africa exhibiting the highest prevalence of these compounds in surface water. This phenomenon can be ascribed to the availability of resources necessary for conducting such detailed research studies in South Africa, resulting in a multitude of studies reporting diverse ARVDs within the country.

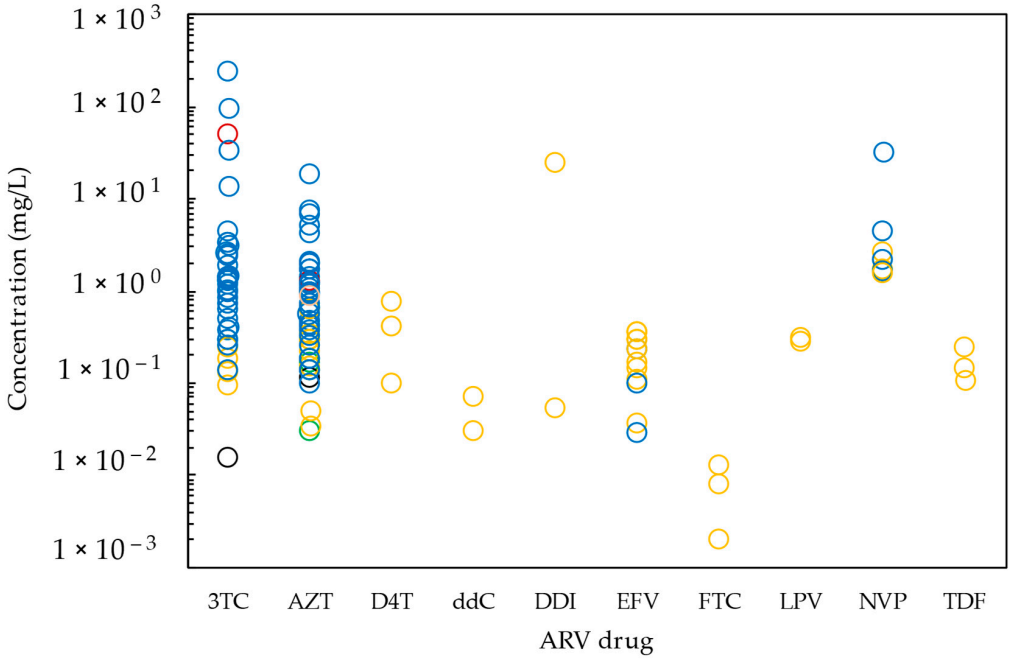

Figure 3. Occurrence of antiretroviral drugs in global surface water matrices, specifically; Belgium (black), Germany (green), Kenya (blue), South Africa (orange), and Zambia (red).

In a research study conducted by Horn et al. [37] in Gauteng, South Africa, the authors concluded that all sampling sites downstream of the investigated WWTPs (Zeekoegat, Olifantsfontein, Flip Human, Vlakplaats, Sunderland Ridge, Welgedacht, and Waterval WWTP) exhibited elevated concentrations of all targeted ARVDs, compared to upstream sampling sites. The dilution of contaminants in surface waters, such as river water, results in ARVDs being detected at reduced concentrations relative to their presence in the effluent [38]. Therefore, the use of dilution factors (DFs) offers a method to estimate probable concentrations of pharmaceuticals in surface waters, in cases where data on consumption, seasonal precipitation, and excretion among others are available [39].

For instance, there is a significant variation in contaminant concentrations between the dry (high) and wet (low) seasons [40]. Furthermore, once introduced into the environment, these drugs undergo numerous processes, including biodegradation, photolysis, and hydrolysis, which may contribute to lower ARVD concentrations in surface waters [41]. Studies conducted in Kenya have reported significantly high concentrations of efavirenz (EFV), lamivudine (3TC), nevirapine (NVP), and zidovudine (AZT) [26,31], in contrast to levels of these pharmaceuticals reported in South Africa [42,43]. For instance, the concentration of EFV detected in River Ngong was measured at 167.10 µg/L [31], while notable concentrations of NVP and AZT were recorded at 5.62 µg/L [5] and 7.68 µg/L [26], respectively, in the same river. In Kenya, 3TC and NVP are utilized as first-line regimen drugs, potentially explaining their elevated concentrations in surface waters [44].

These concentrations originate from runoff in areas lacking sanitation, which is over two million individuals residing along River Ngong near the Nairobi dam [45]. This phenomenon elucidates the disparity in ARVD levels between Kenya and other regions like South Africa, where the concentrations are less than 1 μg/L, despite South Africa operating the most extensive ART programme globally. This discrepancy is predominantly attributed to the differences in sanitation services between developed and developing nations [44]. Elevated ARVD levels in surface waters across Sub-Saharan Africa (SSA) are likely associated with the ART programme as seen in Figure 2 [46] and inadequate sanitation facilities [47]. Consequently, populations in the SSA region, including those undergoing ART, release pharmaceuticals, such as ARVDs, into surface waterways due to insufficient sanitation infrastructure.

3. Risks Associated with Antiretroviral Drugs

3.1. Ecotoxicity of Antiretroviral Drugs

Historically, research has predominantly focused on the toxicity of ARVDs in mammalian systems [48]. It is only recently that studies have started to shed light on the ecotoxicity of these pharmaceuticals, which explains the limited data available on ARVD ecotoxicity [49]. The toxicity of ARVDs toward aquatic organisms, such as fish, algae, daphnia, and bacteria, ranks among the 10 most toxic classes of pollutants [2,6]. For example, Almeida et al. [50] reported that EFV exhibited half maximal effective concentration (EC_{50}) and no observed effect concentration values (NOEC) of 0.026 mg/L and 0.016 mg/L, respectively, following an eight-day exposure to *Ceriodaphnia dubia*. As a result, EFV can be considered extremely toxic to *C. dubia* [50]. Moreover, Robson et al. [51] noted that 0.0103 μg/L of EFV induced significant liver damage and consequently reduced long-chain triglyceride (Lct) levels in *Oreochromis mossambicus* after 96 h exposure, an effect also observed in humans [52].

Similarly, chronic toxicity tests spanning 28 days, conducted by Pitso [53], demonstrated distinctive renal and liver toxicity in *O. mossambicus*. Omotola et al. [54] found that 0.1 mg/L of 3TC resulted in 100% mortality in *Daphnia magna* after 48 h. Furthermore, 8-day chronic toxicity assessments using 3TC on *C. dubia* revealed EC_{50} and NOEC values of 1.345 mg/L and 0.625 mg/L, respectively, highlighting the drug's toxicity to daphnia [50]. Minguez et al. [55] exposed abacavir to *D. magna* and *Pseudokirchneriella subcapitata* for 48 and 72 h, respectively, and determined the EC_{50} values to be > 100 mg/L and 57.32 mg/L, indicating non-harmful and harmful toxicity, respectively. In contrast, AZT was classified as toxic to daphnia (*C. dubia*) with an EC_{50} of 5.671 mg/L [50].

Beyond the scarcity of data on individual drug toxicity, the combined effects of parent drugs and their transformation products (TPs) may demonstrate increased toxicity towards aquatic life [56]. However, data in this domain is critically lacking, despite the widespread use of these drugs in SSA. This situation underscores the necessity for systematic investigations into the toxicity of ARVDs across various biological organizational levels. Given the significant costs and time required to comprehensively assess the risks associated with environmental pollutants, including ARVDs, modelling approaches become essential for predicting their predicted environmental concentrations (PECs) to gauge exposure levels [39]. Additionally, models can be utilized to estimate the aquatic toxicity of most ARVDs via the Ecological Structure Activity Relationships (ECOSAR) (v2.0) software, thereby assisting in the calculation of predicted no-effect concentration (PNEC) values required for risk assessments.

3.2. Ecotoxicological Risk Assessment

The ecological risk assessment (ERA) is executed by calculating the risk quotient (RQ). The RQ is defined as the ratio of measured (predicted) environmental concentrations

(M(P)EC) of a specific chemical within a certain environmental matrix to the PNEC [57,58] for taxa including fish, algae, daphnia, and bacteria, formulated as follows:

$$\mathrm{RQ} = \frac{\mathrm{MEC\ or\ PEC}}{\mathrm{PNEC}} \quad (1)$$

To categorize risk, the framework proposed by Hernando et al. [59] was utilized; this framework has been applied in the assessment of various pharmaceuticals by several researchers, such as Kosma et al. [60], Molnar et al. [61], and Papageorgiou et al. [62]. According to the framework, an RQ < 0.01 indicates that the specific pollutant presents no ecological risk, pollutants with $0.01 \leq \mathrm{RQ} < 0.1$ present low risk, and pollutants with $0.1 \leq \mathrm{RQ} < 1$ present minimal risk, while pollutants with an $\mathrm{RQ} \geq 1$ present high ecological risk.

The PNECs for various matrices are estimated using the effective (lethal) concentration ($\mathrm{E(L)C_{50}}$) values derived from ecotoxicity data for four taxonomic groups: fish, daphnia, algae, and bacteria, coupled with an assessment factor (AF) [59]. Additionally, PNECs derived from species sensitivity distribution curves [61], experimental no observed effect concentrations (NOEC), and $\mathrm{E(L)C_{50}}$ are predominantly used to facilitate the estimation of practical RQ values. Due to the scarcity of published laboratory toxicity data for most ARVDs, as elaborated prior, ECOSAR models, as presented in Figure 4, were applied in the absence of laboratory-generated data [6]. Furthermore, to address the substantial uncertainties linked with toxicity data produced using ECOSAR and $\mathrm{E(L)C_{50}}$ values, AF of 1000 was applied [63]. The PNEC is calculated as shown in Equation (2).

$$\mathrm{PNEC} = \frac{\mathrm{NOEC\ or\ E(L)C_{50}}}{\mathrm{AF}} \quad (2)$$

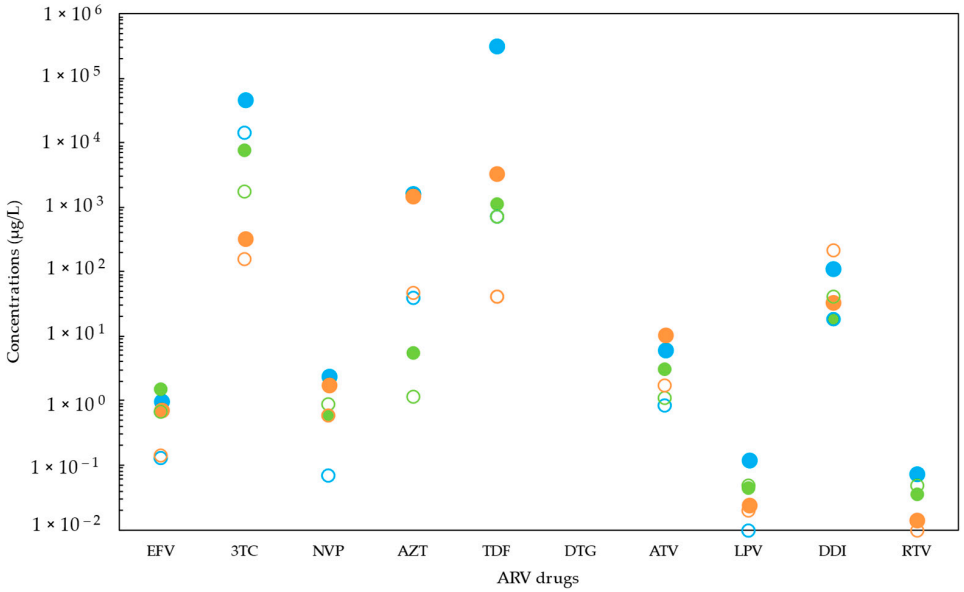

Figure 4. Calculated PNECs for ARVDs using acute (full circle) and chronic (open circles) toxicity data for fish (blue), algae (green), and daphnia (orange).

Currently, reports on the ecological risks of ARVDs are limited, with several illustrative examples being outlined. Ngumba et al. [26] calculated the risk quotients (RQs) for various ARVDs and found that 3TC did not pose a significant risk to aquatic organisms. Conversely, NVP and AZT were found to present ecotoxicological risks to fish, daphnia, and algae in the Nairobi River basin, Kenya. Notably, both ARVDs exhibited the highest risk (RQ > 10) to algae, with NVP showing moderate risk (RQ > 1) to fish and daphnia [26]. Secondly,

efforts by Muriuki et al. [64] to estimate the RQs of 3TC, NVP, and AZT in surface water in Juja, Kenya, resulted in reported RQ values of 0.3, 850, and 1702, respectively.

Due to the lack of specificity regarding aquatic organisms used in the study by Muriuki and colleagues [64], definitive conclusions could not be made. Lastly, Cid et al. [65] assessed the ecological risk of atazanavir (ATV), EFV, and NVP on *Echinometra lucunter* (sea urchin) at Santos Bay, Brazil. Results indicated that EFV posed a high risk (RQ = 4) to the species, while the risk from ATV and NVP was negligible (RQ < 1). In a review by Guo et al. [66], the authors concluded that the risk posed by ATV, 3TC, and NVP to algae was minimal (RQ < 0.01). A similar review by Gani et al. [44], based on three trophic levels, yielded comparable findings, with the RQ of EFV, 3TC, NVP, TDF, zalcitabine, and AZT being less than one, while stavudine distinctly exhibited an RQ greater than ten. According to Reddy et al. [33], the following aquatic species, *Raphidocelis subcapitata*, *Desmodesmus subcapitata*, *Vibro fischeri*, *Artemia salina*, *Skeletonema marinoi*, and *D. magna* are employed as biological models.

3.3. Environmental Risk Characterization

The environmental risk assessment was conducted by quantifying the RQ of various ARVDs across three trophic levels, fish, Daphnia, and algae, using Equation (1). To categorize the varying levels of calculated risk, the framework established by Hernando et al. [59] was utilized, and the findings are illustrated in Figure 4. These findings indicate that ARVDs exhibit highly variable levels of risk to specific or all taxonomic groups in surface water.

Of the seven ARVDs quantified in Gauteng, South Africa, FTC, 3TC, and propargyl ethers from STV concentrations exhibited no threat to any of the three trophic levels assessed in this study. However, EFV and NVP exhibited toxicity ranging from moderate to high among fish, Daphnia, and algae at all locations where these drugs were detected. AZT demonstrated high toxicity towards algae but posed moderate to no significant risk to fish and Daphnia. Carbonyl ureas from STV were found to be highly toxic to algae at all three locations where they were detected, which contradicts Russo et al. [10], who reported that STV had an insignificant impact on algae.

In the Eastern Cape Province, three out of four detected ARVDs, namely TDF, DDI, and ddC, along with their transformation products, displayed an RQ < 1, thereby presenting an insignificant risk to fish, Daphnia, and algae. Conversely, AZT posed no threat to fish and Daphnia but was highly toxic to algae, with an RQ of 94.5. Among the three ARVDs detected and quantified in KwaZulu-Natal (KZN) NVP, EFV, and FTC levels were non-toxic to all three taxonomic groups referenced in this study. Meanwhile, both NVP and EFV exhibited moderate toxicity toward fish and Daphnia while posing minimal risk to algae. This is supported by Reddy et al. [33], who indicate that algae can endure high concentrations of ARVDs in aquatic environments. Further substantiating this, NVP levels posed no risk to algae, whereas EFV was found to be moderately toxic to algae with an RQ of 2.011. In Limpopo, NVP showed moderate toxicity to all species analyzed in this review.

Finally, the MECs of the five ARVDs assessed across seven locations in the Northwest revealed that AZT and ddC exhibited moderate toxicity in fish. In contrast, both TDF anilines and pyrroles at Hartbeespoort Dam were non-toxic. EFV was found to be moderately toxic to fish at the majority of locations, except for the Magalies River, where the risk quotient (RQ) was below 1. Nonetheless, Cayman Chemicals [67] identifies EFV as hazardous to the environment, attributing its persistence and toxicity to aquatic organisms. Robson et al. [51] investigated the acute exposure of 0.0103 µg/L EFV to *O. mossambicus*, determining that EFV inflicted severe hepatic damage, which may lead to future organ loss and overall degradation of fish health. Conversely, NVP ranged from moderate toxicity in fish to presenting no threat to Daphnia and algae, except at Hartbeespoort Dam in 2011 and 2014, where it was moderately toxic. Vogt et al. [68] identified LPV as having the highest

hazard, and our findings corroborate this as the drug exhibited extreme toxicity across all three trophic levels.

Concentrations of 3TC across all three locations in Kisumu, Kenya were found to pose no threat to fish and algae. This is corroborated by the research of Guo et al. [66], which determined the EC_{50} of *P. subcapitata* exposed to 3TC for 72 h to be 96,900 µg/L. Conversely, 3TC exhibited moderate toxicity towards Daphnia in River Ngong and River Kisat, while showing no toxicity in River Auji. AZT, EFV, and NVP, also detected in Kisumu, displayed toxicity ranging from moderate to extreme across all three taxonomic groups, with NVP being the most toxic to fish and Daphnia. In contrast, AZT was identified as the most toxic to algae, with RQ values ranging from 1300 to 2300 across three locations in Kisumu. This aligns with the findings of Russo et al. [10], which showed AZT's higher toxicity to *R. subcapitata*, resulting in approximately 25% growth inhibition.

In Mathare, Kenya, the concentrations of 3TC across all seven locations with reported occurrence data were non-toxic to all trophic levels examined in this review. By contrast, NVP and AZT varied from moderately toxic to extremely toxic, as documented by Ngumba et al. [26], indicating that both NVP and AZT may have potentially ecotoxicological consequences in Daphnia, algae, and fish. AZT concentrations were found to be moderately toxic to fish in most areas within Mathare but exhibited extreme toxicity to fish in the Mathare River near the entrance of the Mathare slum and in Bondeni. Generally, AZT ranged from insignificantly toxic to moderately toxic on algae and Daphnia.

Conversely, NVP demonstrated extreme toxicity to algae in all locations in Mathare, was moderately toxic to fish, and posed no significant risk to Daphnia. In Nairobi, the concentrations of 3TC in all 23 locations were not toxic to any taxonomic groups included in this study. However, the levels of NVP within the Nairobi basin were highly toxic to all three taxa, fluctuating between moderately and highly toxic across the other 22 locations in Nairobi, particularly affecting fish and Daphnia. In European countries, specifically France, Germany, and Poland, the concentrations of ARVDs detected predominantly posed minimal risk (RQ < 10) to all three biomarkers in surface water, with the exception of AZT and STV, which posed the highest acute risk, as depicted in Figure S1, and chronic risk in Figure S2 (RQ > 100) to fish in Germany.

It is apparent that five ARVDs are of primary concern: 3TC, EFV, and NVP due to their high usage; and LPV and RTV because of their very low PNEC values, thereby presenting elevated risks despite their limited use. It should be noted that the risk assessment provided in this study does not accurately reflect the actual risk in the environment. As in complex ecological systems, receptors are exposed to parent ARVDs, their metabolites, and transformation products as mixtures; therefore, the combined effect inevitably enhances the overall risk of these drugs [69]. Additionally, ARVDs like NVP are recognized for their environmental persistence [25]. Collectively, these considerations highlight the substantial and imminent threat that ARVDs present to the environment, emphasizing the pressing need for their effective elimination from surface water matrices.

4. Mechanisms of Photocatalytic Degradation

4.1. Basic Principles of Photocatalytic Degradation Processes

Advanced oxidation processes (AOPs) have been recognized as a notably promising technological method for the degradation of soluble organic contaminants that are present in wastewater matrices. The prevalent chemical characteristic that defines the wide variety of AOPs is their ability to generate reactive oxygen species (ROS), with a particular focus on the hydroxyl radical (•OH), which is recognized as an exceptionally potent oxidizing agent owing to its second highest oxidation potential (2.8 eV) [70]. These reactive species

can be generated in situ and exhibit the capability to oxidize and subsequently mineralize persistent pollutants into benign end products, such as carbon dioxide and water [71].

A variety of AOPs, including Fenton [72], photo-Fenton [73], ozonation [74], ultrasound radiation [75], photolysis [76], and photocatalysis [77], have been employed for the remediation of multiple pharmaceutical pollutants found in wastewater. However, the effectiveness of these methods often shows significant variability depending on the specific type and concentration of the pollutants present. Likewise, tertiary treatment approaches, such as electrodialysis [78], activated carbon adsorption [79], chemical removal [80], coagulation [81], and membrane filtration [82], have been studied for their effectiveness in eliminating pharmaceutical compounds that remain in wastewater following secondary treatment. Despite their implementation, these techniques often demonstrate inconsistent and critically variable removal efficiencies.

Presently, heterogeneous photocatalysis has arisen as one of the most distinguished, comprehensively investigated, and promising AOPs for the efficient removal of persistent contaminants [77]. The process of heterogeneous photocatalysis is initiated when a photocatalyst is irradiated by photons that possess energy that correspond to or exceed its bandgap energy, thereby allowing for the excitation of electrons from the valence band to the conduction band [83]. This excitation phenomenon results in the generation of electron-hole pairs that travel to the surface of the irradiated photocatalyst, where they engage in redox reactions with adsorbed species. Consequently, these reactions culminate in the production of ROS such as •OH and superoxide anions ($O_2\bullet^-$), which play a pivotal role in the oxidative breakdown of organic pollutants. Among the diverse range of photocatalysts, titanium dioxide (TiO_2), particularly the anatase phase and Degussa (a combination of anatase and rutile), stand out as the most extensively researched due to their advantageous characteristics, including high stability, cost-efficiency, and exceptional photocatalytic activity under UV irradiation [84].

Numerous studies have investigated the reaction mechanisms underlying the heterogeneous photocatalysis process using TiO_2 [85]. Figure 5 illustrates the simplified mechanisms for the photoactivation of the semiconductor photocatalyst TiO_2. As depicted in Figure 5, the valence and conduction bands of TiO_2 are separated by a band gap. To initiate the degradation process, TiO_2 requires photoexcitation with light at wavelengths of ca 387 nm for the anatase phase (bandgap of 3.2 eV) and ca 410 nm for the rutile phase (bandgap of 3.0 eV) [86]. In essence, photocatalysis of TiO_2 is initiated by the absorption of photons with energy equal to or greater than its band gap, facilitating the promotion of electrons from the valence band to the conduction band. This transition results in the generation of a positive valence band hole (h^+) and a negative conduction band electron (e^-). Upon irradiation, TiO_2 can function as either an electron donor or molecules acceptor. The powerful oxidant h^+ oxidizes water and hydroxide ions (OH^-) to produce •OH, while the reductant e^- reduces molecular oxygen (O_2) to $\bullet O_2{}^-$. The superoxide radical then reacts with hydrogen ions (H^+) to yield hydrogen peroxide radicals ($\bullet HO_2$), which, upon further protonation by H^+, can produce hydrogen peroxide (H_2O_2). These oxidation and reduction processes occurring on the surface of the photoexcited semiconductor not only generate a plethora of ROS, including •OH, $\bullet O_2{}^-$, $\bullet HO_2$, and H_2O_2, that participate in contaminant degradation but also mitigate the recombination of h^+ and e^-. Equations (3)–(9) outline the key steps involved in the photocatalytic mechanism of TiO_2, including photoexcitation, charge carrier dynamics, and subsequent degradation processes [87].

$$\text{Photoexcitation}: \ TiO_2 + hv \rightarrow e^- + h^+ \tag{3}$$

$$\text{Entrapment of free electrons}: \ e^-_{CB} \rightarrow e^-_{TR} \tag{4}$$

$$\text{Entrapment of free electrons}: \ h^{+}_{VB} \rightarrow h^{+}_{TR} \quad (5)$$

$$\text{Charge carrier recombination}: e^{-}_{TR} + h^{+}_{VB} \rightarrow e^{-}_{CB} + \text{heat} \quad (6)$$

$$\text{Photoexcited electron scavenging}: \ (O_2)_{ads} + e^{-} \rightarrow O_2^{-} \quad (7)$$

$$\text{Oxidation of hydroxyl}: \ OH^{-} + h^{+} \rightarrow \cdot OH \quad (8)$$

$$\text{Photodegradation by hydroxyl radicals}: \ R - H + \cdot OH \rightarrow R' + H_2O \quad (9)$$

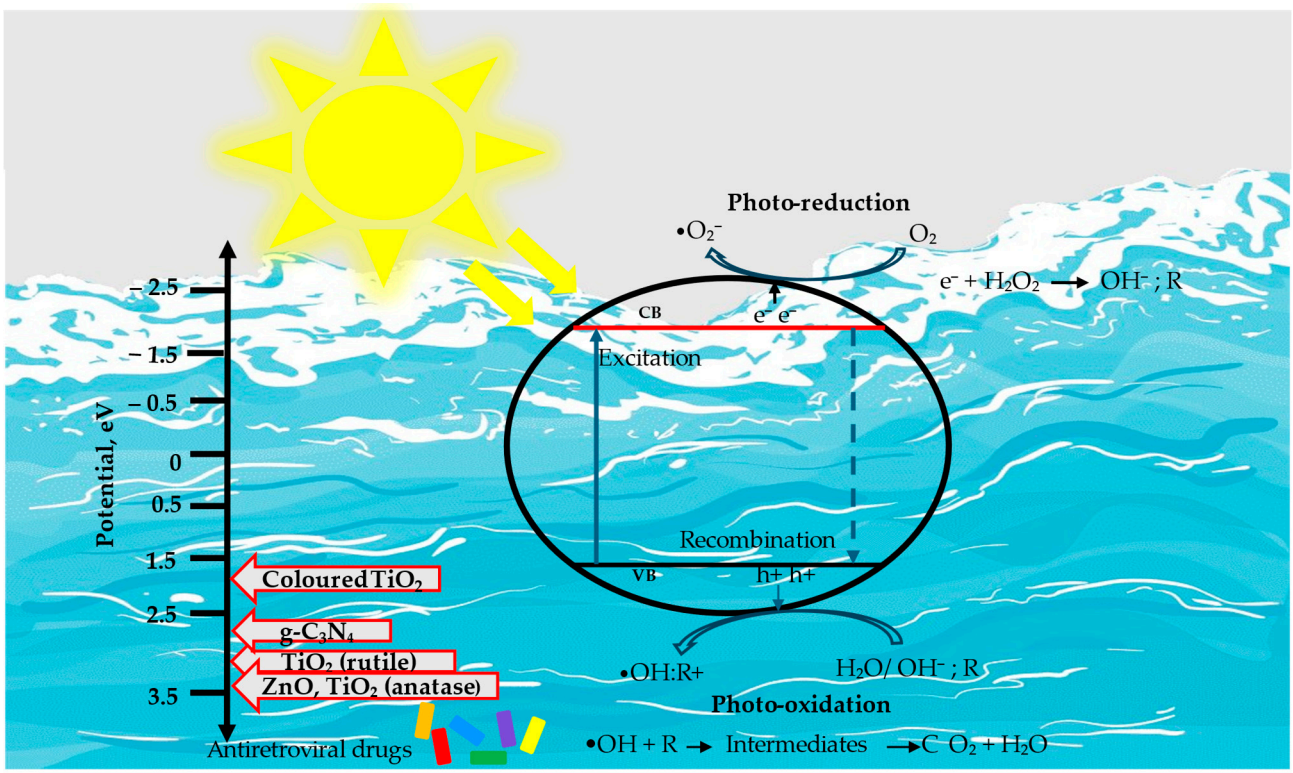

Figure 5. Mechanism for photoactivation of coloured TiO_2, g-C_3N_4, TiO_2, and ZnO semiconductors.

The •OH generated from Equation (8) facilitate the conversion of organic pollutants into intermediate compounds, which are then further degraded through the same reaction pathway until carbon dioxide (CO_2) and water are ultimately produced as the final by-products (Equation (9)). The detailed photocatalytic degradation process consists of various fundamental stages [88]. Initially, organic pollutants are transferred from the bulk liquid phase to the surface of the photocatalyst. Upon arrival at the surface, the pollutants engage in adsorption onto the photon-activated photocatalyst, where the production of reactive oxygen species, including •OH radicals and H_2O_2, triggers the oxidative degradation of the adsorbed contaminants. This mechanism persists until the contaminants are either decomposed into intermediate compounds or entirely mineralized into CO_2 and water. The intermediate or ultimate degradation products are then desorbed from the photocatalyst surface, followed by their transfer back into the bulk liquid phase.

4.2. Factors Influencing the Photocatalytic Degradation of Organic Pollutants

The efficiency of photocatalytic degradation of organic pollutants relies on several operational parameters, with oxidation rates governed by factors such as pollutant properties, catalyst amount, solution pH, surface morphology, reaction temperature, inorganic ions, light intensity, and dissolved oxygen. The pollutant's nature, concentration, and interaction with other compounds in the water matrix significantly influence degradation

rates. For instance, only the pollutants adsorbed on the photocatalyst's surface contribute to degradation, while pollutants in the bulk solution do not. High pollutant concentrations can saturate the photocatalyst's surface, reducing photonic efficiency and potentially deactivating the catalyst [89]. Additionally, the chemical structure of the target pollutant impacts degradation efficiency, as complex compounds, such as 4-chlorophenol, require longer irradiation times due to intermediate transformations before complete mineralization, unlike simpler compounds like oxalic acid [90].

The amount of photocatalyst also plays a vital role in photodegradation efficiency, which increases with catalyst quantity due to the higher number of active sites available for generating •OH that drive the degradation process. However, beyond an optimal amount, further increases can cause turbidity, blocking UV radiation and thereby reducing degradation efficiency [91]. Solution pH alters the surface charge of the photocatalyst and shifts catalytic reaction potentials, affecting pollutant adsorption and reaction rate. Under acidic conditions, TiO_2 surfaces are positively charged, enhancing the adsorption of anionic dyes through Lewis acid-base interactions [92]. Conversely, in alkaline conditions, competitive adsorption by hydroxyl groups and columbic repulsion from the negatively charged surface inhibit dye adsorption. Equations (10) and (11) demonstrate how the surface of Titania can be protonated and deprotonated, respectively. Adsorption is minimal when the solution pH is at the photocatalyst's isoelectric point, where the surface has no net charge.

$$TiOH + H^+ \rightarrow TiOH_2^+ \quad (10)$$

$$TiOH + OH^- \rightarrow TiO^- + H_2O \quad (11)$$

Surface morphology, such as particle size and surface texture, significantly influences photocatalytic degradation, as a larger surface area provides more active sites, enhancing pollutant interaction and degradation efficiency. Nanostructured TiO_2 with grain sizes below 20 nm is particularly effective, as its larger surface area increases the number of active sites. Marin et al. [93] and Pascariu et al. [94] have demonstrated that materials like Cu-TiO_2 nanocomposites exhibit higher degradation rates for organic pollutants compared to TiO_2 due to rough and zigzag surfaces that improve pollutant adsorption. Temperature is another critical parameter, as increased temperatures typically accelerate photocatalytic reactions but also diminish degradation efficiency by disfavouring pollutant adsorption [95]. Reaction temperatures between 20 °C and 80 °C are generally considered ideal for effective photodegradation without excessive recombination.

The presence of inorganic ions, such as magnesium, iron, zinc, and chloride, in wastewater also affects the degradation process by blocking the catalyst's active sites and, in some cases, scavenging reactive species like hydroxyl radicals [96]. While ions such as copper and iron can inhibit photocatalytic efficiency at certain concentrations, ions like calcium and magnesium exhibit minimal inhibition due to their stable oxidation states. Chlorides and other anions (e.g., carbonates, sulphates) can also hinder catalyst activity by decreasing colloidal stability, which diminishes pollutant–catalyst contact and, in turn, reduces degradation efficiency. Some anions, such as chloride, carbonate, and phosphate, act as scavengers for holes and hydroxyl radicals, further inhibiting the photocatalytic process as shown in Equations (12) and (13). Pre-treatment options, such as ion exchange, have been shown to mitigate these inhibitory effects by reducing fouling of the photocatalytic surface.

$$Cl^- + \bullet OH \rightarrow Cl\bullet + OH^- \quad (12)$$

$$Cl^- + h^+ \rightarrow Cl\bullet \quad (13)$$

Light intensity and irradiation time are crucial factors as well. At low light intensities (0–20 mW/cm^2), the degradation rate increases linearly with intensity; at moderate intensities (around 25 mW/cm^2), the rate depends on the square root of light intensity; and at high intensities, it becomes independent, as electron-hole recombination increases and competes with photocatalytic reactions [97]. Dissolved oxygen is typically introduced as an electron acceptor to prevent electron-hole recombination, promoting the stabilization of radical intermediates and aiding in mineralization [98]. It also supports the cleavage of aromatic rings in complex pollutants, ensuring a more efficient breakdown of organic pollutants in aqueous systems.

4.3. Various Photocatalysts Used in the Degradation of Pharmaceuticals

4.3.1. Titanium Dioxide

TiO_2 has emerged as one of the most extensively studied and utilized photocatalysts for the degradation of pharmaceutical pollutants due to its outstanding photochemical stability, non-toxicity, and cost-effectiveness [99]. The advantages of TiO_2 are primarily derived from its capacity to degrade a broad spectrum of organic contaminants when exposed to UV light, whereby it initiates oxidation reactions that decompose pollutants into less harmful by-products [100]. Additionally, TiO_2 is environmentally benign, as it does not generate hazardous by-products during the photocatalytic process [101]. Its anti-microbial properties ensure that TiO_2 can also be used to disinfect water [102]. However, a significant limitation of TiO_2 as a photocatalyst is its high bandgap (~3.2 eV), which confines its activation to ultraviolet (UV) light, a region comprising only a minor part of the solar spectrum [103]. This constraint restricts its practical application in outdoor or natural light settings, necessitating modifications to extend its photocatalytic activity to the visible light spectrum.

To address the limitation of TiO_2's narrow light absorption, various strategies, such as doping with metals and non-metals and forming heterojunctions with other materials, have been employed. Metal doping (e.g., Ag, Cu, and Fe) has been observed to reduce the bandgap of TiO_2 and enhance its charge separation efficiency, resulting in improved photocatalytic performance [104]. Non-metal doping, especially with nitrogen (N) or carbon (C), further enhances its photocatalytic activity under visible light conditions by introducing energy levels within the bandgap that facilitate electron excitation with lower energy light [105]. Furthermore, combining TiO_2 with other materials, such as graphene oxide (GO) and carbon nanotubes (CNTs), has proven effective in improving its charge carrier dynamics and overall photocatalytic efficiency [106].

Despite these advancements, the plausible electron-hole recombination in TiO_2 remains a concern, potentially diminishing its degradation efficiency. The mechanism of TiO_2 photocatalysis in pharmaceutical degradation is predominantly based on the generation of ROS, such as •OH, $\bullet O_2^-$, and hole (h^+) formation upon light exposure [107]. When TiO_2 is irradiated by UV or visible light, electrons are excited from the valence band to the conduction band, creating electron-hole pairs. These charge carriers subsequently interact with water and oxygen molecules on the TiO_2 surface, producing ROS that can attack organic pollutants and break them down into simpler, less toxic compounds [108]. The efficiency of TiO_2 in degrading pharmaceuticals is influenced by several factors, including the type of pollutant, catalyst loading, light source, and environmental conditions such as pH and temperature [109].

Previous studies have documented the degradation of pharmaceutical pollutants through the use of P25 (80% anatase and 20% rutile) as a photocatalyst. In the study, conducted by Wu et al. [110], the authors examined the photocatalytic degradation of TC facilitated by TiO_2 under conditions of both visible light and UV illumination, achieving a removal efficiency of 25.1% and 35.7%, respectively, after an exposure period of

120 min. The observed degradation efficiency under visible light exposure was attributed to the increased sensitivity of TiO_2 induced by TC, which facilitated the formation of a surface complex conducive to visible light absorption. Furthermore, the generation of $\bullet O_2^-$ species as a result of the photoexcitation of the surface complex was identified as pivotal in the photocatalytic degradation occurring under visible light. Conversely, the degradation facilitated by UV irradiation was attributed to the higher energy levels associated with UV photons and the significant roles played by the active species $\bullet O_2^-$ and h^+ a in the process. In another study, Yang et al. [111] employed TiO_2 for the photocatalytic degradation of sulfachlorpyridazine, sulfapyridine, and sulfisoxazole, achieving removal efficiencies of 85.2%, 92.5%, and 85.0%, respectively, following 60 min of UV light exposure. The researchers ascribed the high removal rates primarily to h^+ and •OH, noting that other ROS contribute insignificantly to the degradation process.

4.3.2. Black Titanium

Since its discovery in 2010, hydrogenated coloured titanium (coloured TiO_2) has been utilized for the degradation of numerous pollutants, achieving remarkable degradation in the shortest possible time [22]. Under visible and infrared irradiation, the presence of oxygen vacancies in the material influences the recombination efficiency of photogenerated electron-hole pairs, thereby extending the carrier lifespan and enhancing photocatalytic performance [112]. For instance, Zou et al. [113] attributed the tenfold increase in the photocatalytic evolution rate in coloured TiO_2 to hydrogen-induced oxygen vacancies, which promote the separation and transfer of electron-hole pairs. In a study by Qiang et al. [114], a 0.5% RuTe2/B-TiO_2 catalyst calcined at 400 °C demonstrated exceptional degradation performance, with Zeng et al. [115] attributing this to the crystal structure of coloured TiO_2 achieved at 400 °C. Similarly, Andronic et al. [116] observed that colouredTiO_2 reduced by NaBH4 and calcined at 400 °C was the most effective photocatalyst, achieving 100% degradation of amoxicillin (AMX).

Interestingly, the catalytic dosage of coloured TiO_2 is not inherently advantageous. According to Qiang and colleagues' [114] observations, increasing the catalytic dosage from 20 to 40 and 80 mg diminishes the degradation rate of diclofenac (DCF). This result is attributed to reduced light transmission caused by turbidity induced by the catalyst [117,118]. Additionally, the pH of the reaction system serves an auxiliary but essential function in dictating the catalytic efficacy and stability of semiconductor-based photocatalysts. Influencing particle stability and aggregation, Fermi-level shifts, which determine the reduction potentials of electrons and band-edge positions, and lastly, the electrostatic interactions of electron donors and acceptors. The pH dictates the surface charge of the photocatalyst, which is governed by its point of zero charge (PZC). At pH values below PZC, the surface of the photocatalyst assumes a positive charge, thereby promoting the adsorption of negatively charged species (anions). In contrast, at pH values above the PZC, the surface acquires a negative charge, which favours the adsorption of positively charged species (cations). Effective adsorption amplifies the interaction between the pollutant and reactive species, thereby enhancing the degradation efficiency [119].

Numerous pharmaceutical pollutants show pH-dependent speciation attributable to the presence of functional groups such as carboxylic acids and amines. At varying pH levels, the ionization state of these groups is altered, influencing their interaction with the photocatalyst surface. For example, ionized forms may exhibit stronger adsorption on surfaces with opposite charges, leading to increased degradation [120]. The formation of ROS, particularly •OH, is contingent on pH. At lower pH values, radical protonation may occur, diminishing their reactivity. In contrast, within a pH range of 6 to 8, OH^- can be transformed into ·OH radicals by oxidation, thus improving degradation rates. Consequently, optimal pH for photocatalytic degradation frequently balances ROS generation

and pollutant adsorption [121]. Extreme pH values can deactivate active sites on the photocatalyst by instigating surface corrosion or precipitate formation, such as hydroxides, which obstruct reactive sites. Therefore, maintaining an appropriate pH range is paramount for sustainable photocatalytic activity [122].

In the study by Sarafraz et al. [123], the degradation of ciprofloxacin (CIP) using coloured TiO_2 showed a slight increase with rising pH, reaching its optimal degradation at approximately pH 6.7. The authors accredit this performance to CIP's existence in a zwitterionic form at neutral pH ranges, which enables increased electrostatic interactions between CIP and the positively charged coloured TiO_2, therefore concomitantly enhancing the rate of reaction. The improved photocatalytic degradation at a neutral pH was further ascribed to the hydrophobic interactions, as zwitterionic CIP is highly hydrophobic in nature [124].

4.3.3. Zinc Oxide

Zinc oxide (ZnO) is extensively employed as a photocatalyst in various photocatalytic processes pertinent to water treatment applications [125]. Functioning as an n-type semiconductor, ZnO is characterized by a substantial exciton binding energy of 60 meV and a broad bandgap of 3.2 eV at ambient temperature [126]. Moreover, it demonstrates remarkable photochemical stability, piezoelectric characteristics, and biocompatibility [127]. Given that its bandgap is nearly equivalent to that of TiO_2, as seen in Figure 5 the photocatalytic efficiencies of these two materials are anticipated to be similar [128]. However, parameters such as morphology, charge-transfer kinetics, and surface interactions can considerably influence the efficacy of semiconductors in photocatalytic applications [129]. ZnO exhibits superior electron mobility, approximately 10 to 100 times greater than that of TiO_2, coupled with an elevated quantum yield, rendering it an efficient catalyst and a viable alternative to TiO_2 [128]. The augmented electron mobility of ZnO is particularly advantageous when the catalyst operates as an electron acceptor, thereby facilitating the transfer of electrons from photoexcited organic pollutants to dissolved oxygen under visible light irradiation [130]. In this process, the excited organic molecules transfer electrons to the conduction band of the catalyst, while the organic pollutants themselves are converted into their respective cationic radicals. The injected electrons subsequently engage in reactions with oxygen adsorbed on the surface of the catalyst, leading to the formation of reactive oxygen species such as $\bullet O_2^-$, H_2O_2 and OH• [131].

Several studies have indicated superior removal efficiencies for ZnO in comparison to TiO_2 under designated operational parameters [128,132]. For example, Han et al. [133] illustrated that, when subjected to optimized operational conditions, the UV/ZnO combination exhibits markedly enhanced efficacy relative to the UV/TiO_2 in the decontamination of pharmaceutical compounds. The mechanism that governs the photocatalytic process in the presence of UV light is based on the excitation of the semiconductor through photon absorption, assuming that the photon energy is compatible with or exceeds its bandgap. This leads to the promotion of electrons from the valence band to the conduction band, generating electron-hole pairs as shown in Equation (14). Equations (14)–(18) describe the key steps involved in the photocatalytic degradation process using ZnO, including the generation of charge carriers, the formation of reactive oxygen species, and the oxidation of organic matter.

$$ZnO + h\nu \rightarrow ZnO\left(h_{\nu b}^{+} + e_{cb}^{-}\right) \quad (14)$$

$$e_{cb}^{-} + O_2(ads) \rightarrow \bullet O_2^{-} \quad (15)$$

$$h_{\nu b}^{+} + H_2O(ads) \rightarrow H^{+} + \bullet OH \quad (16)$$

$$h_{\nu b}^{+} + OH^{-}(ads) \rightarrow \bullet OH \quad (17)$$

$$h^{+}_{vb} + \text{organic matter(OM)} \rightarrow OM^{+} + \text{oxidized products} \quad (18)$$

The electron-hole pairs produced during the photocatalytic mechanism have the potential to either engage in direct reactions with organic contaminants (Equation (18)) or indirectly trigger the generation of reactive radicals (Equations (15)–(18)), which subsequently facilitate the degradation of organic substances. Under optimal operational conditions, organic pollutants can undergo complete mineralization into carbon dioxide, water, and harmless anions. However, in some cases, complete mineralization remains unattained, resulting in the formation of intermediate by-products. A key drawback of ZnO photocatalysts lies in the fast recombination of photogenerated electron-hole pairs, which adversely impacts their overall efficiency [125]. As a result, structural modifications to ZnO, intended to augment its activity under visible light, may present a promising and sustainable strategy for enhancing its performance. Such developments could position ZnO as a potent photocatalyst for a diverse array of environmental applications. Several cases of ZnO used in the degradation of pharmaceuticals have been reported. For example, Ravbar et al. [134] illustrated that ZnO, synthesized utilizing an ethanolic extract from the roots of Japanese knotweed, effectively facilitated the degradation of ciprofloxacin (CIP), attaining a degradation efficiency of 100%. Similarly, Vigmanti et al. [80] reported on the complete elimination of spiramycin and ofloxacin (OFL), while Zhang et al. [135] exhibited the total degradation of metronidazole, all employing ZnO in the capacity of a photocatalyst.

4.3.4. Graphitic Carbon Nitride-Based Photocatalysts for the Removal of Pharmaceutical Contaminants

Graphitic carbon nitride (g-C_3N_4) is an eco-friendly and cost-effective metal-free semiconductor photocatalyst known for its high physicochemical stability and favourable electronic properties, including a medium band gap of 2.7 eV [136]. Its unique attributes, such as a high mesoporous volume, large surface area, conjugated porous polymeric structure, visible light responsiveness, and strong adsorption capacity, make it a promising candidate for the catalytic removal of hazardous organic pollutants from aqueous environments. Structurally, g-C_3N_4 consists of two-dimensional sheets of tris-s-triazine units connected via tertiary amines and can be synthesized from widely available materials, including dicyandiamide, cyanamide, melamine, urea, and thiourea, through calcination at elevated temperatures [137]. Research indicates that the choice of precursor significantly influences the properties of g-C_3N_4. For example, a study by Attri et al. [138] and Nejad et al. [139] examined how precursors such as cyanamide, melamine, urea, and thiourea affect the photophysical properties of g-C_3N_4 for tetracycline (TC) degradation under visible light. The photocatalytic efficiency followed the following order: urea-derived g-C_3N_4 (U-CN) > thiourea-derived g-C_3N_4 (T-CN) > cyanamide-derived g-C_3N_4 (C-CN) > melamine-derived g-C_3N_4 (M-CN). Urea-derived g-C_3N_4 demonstrated superior photocatalytic activity, which was attributed to its high surface area and reduced charge carrier recombination. Upon exposure to visible light, photogenerated electrons in the conduction band of g-C_3N_4 react with molecular oxygen to form $\bullet O_2^{-}$, which, together with holes in the valence band, decompose tetracycline molecules, as demonstrated by studies using radical scavengers such as isopropanol, $AgNO_3$, benzoquinone, and triethanolamine.

Various studies have explored the degradation of pharmaceutical pollutants using g- C_3N_4. For instance, polymeric g-C_3N_4 synthesized via the polycondensation of melamine was found to degrade pharmaceuticals like tetracycline, ciprofloxacin, salicylic acid, and ibuprofen under UV-visible light irradiation [140]. The polymeric g-C_3N_4 exhibited better degradation efficiency for tetracycline (86%) and ciprofloxacin (60%) compared to salicylic acid (30%) and ibuprofen (20%) in acidic conditions. The mineralization order for these drugs was tetracycline > salicylic acid > ciprofloxacin > ibuprofen. Recent studies

have provided insights into the enhanced photodegradation of pharmaceuticals, including naproxen (NPX), indomethacin (IDM), diclofenac (DCF), carbamazepine (CBZ), triclosan (TCS), ofloxacin (OFX), enrofloxacin (ENR), and sulfamethoxazole (SME), by improving the crystallinity of g-C_3N_4 [141]. The improved crystallinity facilitates oxygen absorption and promotes direct oxygen reduction through a two-electron pathway, leading to increased H_2O_2 production and more hydroxyl radicals, which aid in the decomposition of pharmaceuticals, as supported by experimental and computational analyses.

Despite its advantages, g-C_3N_4 suffers from limitations such as a high recombination rate of photogenerated charge carriers and a low specific surface area, which reduce its photocatalytic efficiency. Several approaches have been employed to address these drawbacks, including the introduction of vacancy defects and heteroatoms [69], metal and non-metal doping [126], and coupling with narrow bandgap semiconductors [142].

4.3.5. Composite Photocatalysts for Application in Remediation of Pharmaceuticals

The advancement of heterogeneous photocatalysis has seen significant progress through the development of photocatalysts that are environmentally sustainable, cost-effective to synthesize, responsive to visible light, and possess enhanced durability. These advancements are often achieved through modifications such as doping and sensitization of conventional photocatalysts, as well as fabricating novel heterojunction photocatalysts by combining regular photocatalysts. Notably, doping with metal ions or co-doping with metals and non-metals, along with modifying metal oxides using capping agents, have proven to be effective strategies to minimize charge carrier recombination. For example, Pazoki et al. [143] investigated the degradation of dexamethasone using a TiO_2/Ag photocatalyst under visible and UV light irradiation, achieving a degradation efficiency of 82.3% under UV and 71.5% under visible light. Similarly, co-doped (Ag, Cu) TiO_2 photocatalysts synthesized via the sol–gel method achieved a 98% removal efficiency of acyclovir, which was 2.34 times greater than that of pure TiO_2.

Heterojunction semiconductors have gained attention as a promising method for improving photocatalytic systems, particularly in optimizing visible light utilization. Graphene oxide (GO), due to its two-dimensional structure, large surface area, and excellent conductivity, is highly effective in enhancing photocatalytic performance through pollutant adsorption, charge separation, and extended light absorption. Evgenidou et al. [144] synthesized GO-TiO_2 nanocomposites and reported high photocatalytic efficiency for abacavir degradation, with a composite containing 2% GO completely degrading the compound within just 20 min.

In another study, a composite photocatalyst of TiO_2 nanoparticles and multi-walled carbon nanotubes (TNPs–MWCNTs) was synthesized using a soft-template hydrothermal method, with its composition optimized through a central-composite design (CCD) approach [145]. Under optimal conditions, this composite demonstrated a remarkable acyclovir degradation efficiency of 98.6%. Ayodhya [146] developed a Z-scheme catalyst, CuO@Ag@Bi2S3, achieving 92.14% stavudine removal within 30 min, and 87.4% for zidovudine. The superior efficiency is attributed to the enhanced adsorption capacity and the presence of active species such as $\bullet O_2^-$ and holes (h^+) during the photocatalytic process.

Bhembe et al. [147] synthesized an FL-BP@Nb2O5 photocatalyst and demonstrated enhanced NVP degradation due to the reduction in bandgap at the BP-Nb_2O_5 interface, which promoted electron migration and surface reactivity. Optimized conditions revealed that the lowest NVP concentration (5 ppm), with a catalyst loading of 15 mg at pH 3, resulted in the highest degradation efficiency. Tabana et al. [148] investigated the removal of EFV and NVP using an Ag-AgBr-LDH composite photocatalyst. Using response surface methodology (RSM), they identified significant interactions between photocatalyst loading,

initial pollutant concentration, and pH, as summarized in Figure 6. The study demonstrated over 80% degradation of EFV and 100% degradation of NVP under neutral pH and visible light within 12 and 8 h, respectively. A summary of heterojunction semiconductor performances for the degradation of ARVDs and other pharmaceuticals is presented in Table 2.

Table 2. Degradation of pharmaceutical contaminants using heterojunction semiconductor photocatalysts.

Pharmaceutical	Photocatalyst	Catalyst Dosage (g/L)	Irradiation	Removal Efficiency (%)	Reference
3TC	P25	1	365 UV	>95	[147]
ABC	GO-TiO_2	0.1	500 W m^{-2}	99	[142]
ACE	Black TiO_2	3	UV	99	[148]
ACE	OVPTCN	0.5	Visible: 300 W Xe lamp	96	[149]
ACV	TNPs-MWCNTs	0.02	125 W Hg lamp	98.6	[143]
ACV	g-CN/TiO_2	0.03	300 W Xe lamp	100	[150]
ACV	Ag_2MoO_4/g-C3N_4	0.25	300 W Xe lamp	100	[151]
ACV	Bi4VO_8Cl	1	300 W Xe lamp	100	[152]
ACV	TNPs-MWCNTs	0.4	365	98	[143]
ACV	g-CN/TiO_2	0.3	>420	100	[150]
ACV	Ag_2MoO_4/g-C_3N_4	0.25	>420	100	[151]
ACV	BiVO_8Cl	0.05	200–700	100	[152]
AMX	Black TiO_2	0.6	F18W/T8, UVA	100	[116]
AMX	AC/TixOy	0.01	100 W/m2 LED lamp	92	[153]
Antipyrine	Defective-TiO_2	0.01	Visible: 36 W lamp	100	[154]
Arbidol Hydrochloride	Ti_3C_2MXene/g-C_3N_4	0.1	>420	99	[155]
AZT	5%BZONPs	0.1	8 W UV lamp	100	[156]
AZT	CuSm0.06Fe1.94O_4@g-C_3N_4	0.12	Visible	71.5	[157]
AZT	CuO@Ag@Bi_2S_3	0.02	200 UV-A	87.4	[144]
AZT	CuSm0.06Fe1.94O_4@g-C_3N_4	1.2	>420	72	[157]
AZT	CuO@Ag@Bi_2S_3	0.02	200 UV-A	87	[144]
Carbamazepine	BTN@PCs	0.6	Visible: Xe lamp	63	[158]
CIP	CSs/TiO_2-x@gC_3N_4	1	Visible: 1000 W Xe lamp	90	[159]
CIP	BTN@PCs	0.6	Visible: Xe lamp	84	[123]
DCF	RuTe2/B-TiO_2	0.3	250W Xe lamp	95.2	[158]
Doxycycline Hydrochloride	RGO/BTiO_2/2D-ZIF-8	0.1	Visible: 300 W Xe lamp	76	[114]
EFV	Ag-AgBr-LDH	2		84	[160]
IBP	B-N-TiO_2	0.4	Visible: 5 W LED lamp	96	[146]
LPV	Ammonium molybdate (WU and WW photocatalysts)	0.4	500–550	95	[123]
LVFX	NTTC	0.3	Visible: Xe lamp	~60	[161]
Norfloxacin	BTN@PCs	0.6	Visible: Xe lamp	45	[162]
NVP	FL-BP@Nb_2O_5	0.1	>420	68	[158]
NVP	Ag-AgBr-LDH	2		100	[145]
Oseltamivir	P25	0.5	365 UV	96	[146]
Oxytetracycline	BTN@PCs	0.6	Visible: Xe lamp	94	[163]
Oxytetracycline Hydrochloride	Dark brown TiO_2 spheres		Natural sunlight	80	[158]
PAR	AC/TixOy	0.01	100 W/m^2 LED lamp	100	[164]
RBV	Bi_4VO_8Cl	0.05	200–780	100	[153]
RTV	(WU and WW photocatalysts)	0.4	500-550	95	[152]
STV	CuO@Ag@Bi_2S_3	0.02	200 UV-A	92.1	[161]
Sulfisoxale	C-doped TiO_2-x	0.4	Visible: CEL–HXF300 Xe lamp	~70	[144]
Sulfisoxale	BTN@PCs	0.6	Visible: Xe lamp	75	[165]
TC	Black anatase-TiO_2	0.2	Visible: 1000 W Xe lamp	66.2	[158]
TC	γ-Fe2O_3/b-TiO_2	0.3	Solar: 300 W Xe lamp	99.3	[166]
TC	BTN@PCs	0.6	Visible: Xe lamp	90	[167]
TC	RGO@BT	0.2	Solar	94	[149]
TC	Ag/La-TiO_2-x	0.5	300 W Xe	98	[168]

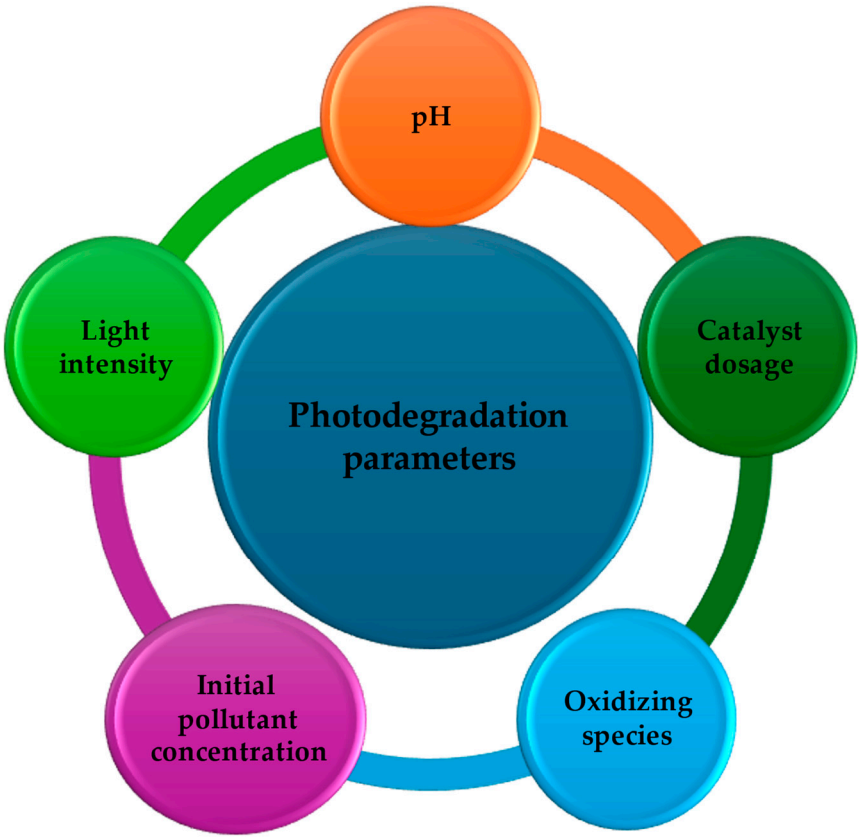

Figure 6. Factors influencing the photocatalytic degradation efficiency of variant contaminants.

5. Challenges and Limitations

The principal challenge in the application of photocatalytic technologies for wastewater treatment is scalability [169,170]. Although all the aforementioned photocatalysts exhibit exceptional photocatalytic activity in laboratory-scale investigations, their efficacy is markedly diminished in extensive, real-world scenarios. Factors such as light penetration, mixing efficiency, and the surface area of the photocatalyst become increasingly complex at larger scales, posing difficulties in achieving consistent photocatalytic reactions [112,171]. Furthermore, the degradation of pharmaceuticals in real wastewater, which contains complex mixtures of organic and inorganic substances, can hinder photocatalytic performance due to interference from co-contaminants and light-blocking materials [172,173].

The economic feasibility of photocatalytic degradation versus conventional treatment methodologies continues to pose a substantial impediment to its extensive implementation [174]. Conventional treatment approaches, such as activated carbon adsorption, ozonation, and biological treatments, are well-established, cost-effective, and more facile to deploy on a large scale [175]. Conversely, the production of advanced photocatalysts, like ZnO, frequently entails the use of costly materials and processes that demand considerable energy [176]. Additionally, the requirements for ultraviolet or visible light sources to activate these photocatalysts can escalate operational expenditures, particularly in regions with limited sunlight exposure. Consequently, the equilibrium between material costs, energy consumption, and overall operational expenses in contrast with environmental advantages persists as a challenge.

A significant challenge in the application of photocatalysts lies in their temporal stability [177]. The deactivation of photocatalysts may result from the accumulation of reaction intermediates on the catalyst surface [112], which occludes active sites, thus reducing the efficiency of the photocatalyst [178]. This issue is particularly pronounced in

the degradation of pharmaceuticals, wherein complex organic molecules can form fouling layers on the catalyst [179]. Regeneration strategies, including thermal treatment or chemical washing, may restore activity but can also induce structural alterations or leach active components, thereby diminishing the catalyst's long-term viability [180]. Consequently, achieving stable photocatalytic performance with minimal regeneration demands remains a persistent research challenge.

6. Future Research Directions

A significant research gap in the photocatalytic degradation of pharmaceuticals, particularly ARVDs, lies in the insufficient understanding of the degradation pathways and resultant by-products. Although studies have validated the effectiveness of photocatalysts such as coloured TiO_2, ZnO, and others in degrading ARVDs, the identification of toxic intermediates, even more toxic than the parent drugs [181] raises concerns as these degradation products remain largely unexplored. This understanding is essential to ensure that the photocatalytic process does not result in the formation of harmful by-products. Furthermore, the photocatalytic efficiency in real wastewater matrices, where the presence of organic matter and other contaminants may impede the degradation process, warrants further investigation. The long-term stability and reusability of these photocatalysts also necessitate greater attention, particularly within continuous flow systems.

The advancement of novel and more efficient photocatalysts is crucial for progression in this domain. Ongoing research on doped or modified catalysts, such as coloured TiO_2 and composites with graphene or other carbon-based materials, demonstrates potential in augmenting visible-light absorption and charge separation, thereby enhancing photocatalytic performance. Future innovations may entail the exploration of hybrid catalysts that integrate semiconductor materials like ZnO with plasmonic metals or co-catalysts to improve both light absorption and degradation kinetics. Furthermore, the development of photocatalysts with tenable surface properties capable of selectively degrading pharmaceuticals without interference from other wastewater contaminants represents a promising avenue for future research.

Another key challenge lies in integrating photocatalytic systems into existing wastewater treatment frameworks. Although photocatalysis demonstrates efficacy in degrading pharmaceuticals such as ARVDs, it is crucial to amalgamate it with traditional methodologies including biological treatment, filtration, or adsorption to augment the overall treatment efficiency. Prospective research should emphasize the optimization of hybrid systems that incorporate photocatalysis as a polishing step or as an element of a multi-stage process, ensuring the comprehensive removal of both parent compounds and degradation by-products. Furthermore, achieving cost-effective scalability of photocatalytic systems for practical use requires the development of innovative reactor designs that can handle large volumes of wastewater under natural sunlight or low-energy artificial lighting.

7. Conclusions and Recommendations

7.1. Conclusions

The environmental persistence of ARVDs in aquatic matrices highlights the urgent need for advanced remediation technologies. These pharmaceuticals, including EFV, 3TC, and NVP, culminate in the environment due to incomplete human metabolism and inadequate removal by conventional WWTPs, posing ecotoxicological risks to aquatic organisms and plausible human health impacts. Risk quotient analyses reveal elevated toxicity levels in several regions, with the SSA region, particularly for EFV and NVP, necessitating urgent intervention. Photocatalysis emerges as a viable solution, with coloured TiO_2, ZnO, and various carbon-based composites demonstrating superior performance due to their modi-

fied bandgap structure, which enhances visible and infrared light absorption compared to pristine TiO_2. This property, combined with improved charge separation efficiency and stability under prolonged illumination, position these photocatalysts as leading candidates for scalable applications. Coloured TiO_2 in particular possesses substantial potential for the remediation of ARVDs in wastewater; its cost-effectiveness, facilitated by boron doping, and compatibility with hybrid treatment systems further strengthen its potential for integration into existing infrastructure.

While laboratory studies highlight coloured TiO_2's efficacy in degrading ARVDs, challenges persist in translating these findings to real-world scenarios. A major concern involves the incomplete elucidation of degradation pathways and the potential formation of toxic transformation products, which could exacerbate secondary pollution. Additionally, reactor design limitations, such as inefficient light penetration and catalyst dispersion in complex wastewater matrices, require optimization to ensure practical viability. Synergistic approaches combining photocatalysis with biological treatment, adsorption, and membrane filtration may enhance degradation efficiency. Coloured TiO_2's stability and prolonged lifespan under solar irradiance make it particularly suitable for multi-stage systems, especially in regions with abundant sunlight. This review bridges the gap between laboratory innovation and practical implementation, emphasizing the urgency of advancing catalyst design, reactor engineering, and integrated treatment strategies. Through sustained interdisciplinary efforts, photocatalysis, particularly coloured TiO_2 holds transformative potential to mitigate ARVD contamination, safeguarding both aquatic ecosystems and human health. By addressing these challenges, society can transition from experimental success to scalable solutions, ultimately reducing the environmental burden of pharmaceutical pollutants and fostering sustainable water management practices.

7.2. Recommendations

Future research should focus on addressing the existing gaps in understanding degradation mechanisms and their by-products, particularly in real wastewater scenarios. The identification and assessment of the toxicity of degradation intermediates are crucial to ascertain those photocatalytic methodologies do not inadvertently generate deleterious compounds. Furthermore, the pursuit of more efficient, resilient, and economically viable photocatalysts continues to be a significant research imperative. The exploration of hybrid catalysts that merge semiconductor materials with plasmonic metals or different co-catalysts shows significant potential for advancing photocatalytic capability under visible light conditions. In addition, the development of this technology and the integration of photocatalytic processes in hybrid treatment systems will require significant advancements in reactor design and methodologies for process optimization. Concurrently, regulatory frameworks must evolve to mandate advanced treatment technologies for pharmaceutical pollutants, ensuring proactive environmental stewardship. The integration of photocatalysis into multi-stage treatment systems that incorporate conventional methods such as biological treatment and adsorption holds considerable promise for substantially improving the overall effectiveness and practicality of removing pharmaceutical pollutants. Ultimately, achieving a balance between performance indicators and operational costs, notably in regions with scarce solar radiation, is key to realizing the full potential of photocatalysis in wastewater treatment globally.

Supplementary Materials: The following supporting information can be downloaded at: https://www.mdpi.com/article/10.3390/catal15040381/s1, Figure S1: Acute risk characterization of ARVDs (nevirapine (green), zidovudine (orange), lamivudine (blue), efavirenz (yellow), emtricitabine (grey), stavudine (red), tenofovir (purple), zalcitabine (brown), didanosine (pink), lopinavir (black), darunavir (green open circles), ritonavir (blue open circles), and abacavir (orange open circles))

obtained using measured concentrations in surface waters across the globe (F—France, G—Germany, K—Kenya, P—Poland, S—South Africa, and Z—Zambia) relative to no-effect concentrations for (a) fish, (b) algae, and (c) daphnia taxonomical groups. And Figure S2: Chronic risk characterization of ARVDs (nevirapine (green), zidovudine (orange), lamivudine (blue), efavirenz (yellow), emtricitabine (grey), stavudine (red), tenofovir (purple), zalcitabine (brown), didanosine (pink), lopinavir (black), darunavir (green open circles), ritonavir (blue open circles) and abacavir (orange open circles)) obtained using measured concentrations in the surface water across the globe (F—France, G—Germany, K—Kenya, P—Poland, S—South Africa, and Z—Zambia) relative to no-effect concentrations for (a) fish, (b) algae, and (c) daphnia taxonomical groups.

Author Contributions: Conceptualization, writing—original draft preparation, P.N.; writing, reviewing and editing P.N. and L.S.T.; writing, reviewing and editing, and supervision, E.M.N.C. and S.M.T. All authors have read and agreed to the published version of the manuscript.

Funding: This research was funded by the National Research Foundation of South Africa (NRF) through Grants Number: EQP180503325881 awarded to E.M.N. Chirwa, and NRF Grant Number: CSRP2304239632 awarded to S.M. Tichapondwa, both at University of Pretoria.

Data Availability Statement: Not applicable.

Acknowledgments: During the preparation of this manuscript, the authors used Grammarly and Writefull for the purposes of text editing (e.g., grammar, structure, spelling, punctuation, and formatting. The authors have reviewed and edited the output and take full responsibility for the content of this publication.

Conflicts of Interest: The authors declare no conflicts of interest.

References

1. Kümmerer, K. Pharmaceuticals in the Environment. *Annu. Rev. Environ. Resour.* **2010**, *35*, 57–75. [CrossRef]
2. Kümmerer, K. The Presence of Pharmaceuticals in the Environment Due to Human Use—Present Knowledge and Future Challenges. *J. Environ. Manag.* **2009**, *90*, 2354–2366. [CrossRef] [PubMed]
3. Weber, F.-A.; aus der Beek, T.; Bergmann, A.; Carius, A.; Grüttner, G.; Hickmann, S.; Ebert, I.; Hein, A.; Küster, A.; Rose, J.; et al. *Pharmaceuticals in the Environment—The Global Perspective*; German Environment Agency: Berlin, Germany, 2014.
4. Health Care Without Harm a Multi-Stakeholder Approach to Pharmaceuticals in the Environment: Working Together Towards Effective Solutions. Available online: https://europe.noharm.org/resources/multi-stakeholder-approach-pharmaceuticals-environment-working-together-towards-effective (accessed on 17 April 2024).
5. Date, M.; Jaspal, D. Pharmaceutical Wastewater Remediation: A Review of Treatment Techniques. *Ind. Eng. Chem. Res.* **2023**, *62*, 20492–20505. [CrossRef]
6. Sanderson, H.; Johnson, D.J.; Reitsma, T.; Brain, R.A.; Wilson, C.J.; Solomon, K.R. Ranking and Prioritization of Environmental Risks of Pharmaceuticals in Surface Waters. *Regul. Toxicol. Pharmacol.* **2004**, *39*, 158–183. [CrossRef] [PubMed]
7. Xu, D.; Xie, Y.; Li, J. Toxic Effects and Molecular Mechanisms of Sulfamethoxazole on *Scenedesmus obliquus*. *Ecotoxicol. Environ. Saf.* **2022**, *232*, 113258. [CrossRef] [PubMed]
8. Gupta, V.K.; Thakker, A.; Gupta, K.K. Vestibular Schwannoma: What We Know and Where We Are Heading. *Head Neck Pathol.* **2020**, *14*, 1058–1066. [CrossRef]
9. Wang, X.; Wu, Q.; Liu, A.; Anadón, A.; Rodríguez, J.-L.; Martínez-Larrañaga, M.-R.; Yuan, Z.; Martínez, M.-A. Paracetamol: Overdose-Induced Oxidative Stress Toxicity, Metabolism, and Protective Effects of Various Compounds in Vivo and in Vitro. *Drug Metab. Rev.* **2017**, *49*, 395–437. [CrossRef]
10. Russo, D.; Siciliano, A.; Guida, M.; Andreozzi, R.; Reis, N.M.; Li Puma, G.; Marotta, R. Removal of Antiretroviral Drugs Stavudine and Zidovudine in Water under UV254 and UV254/H_2O_2 Processes: Quantum Yields, Kinetics and Ecotoxicology Assessment. *J. Hazard. Mater.* **2018**, *349*, 195–204. [CrossRef]
11. Akhtar, Z.R.; Tariq, K.; Mavian, C.; Ali, A.; Ullah, F.; Zang, L.-S.; Ali, F.; Nazir, T.; Ali, S. Trophic Transfer and Toxicity of Heavy Metals from Dengue Mosquito Aedes Aegypti to Predator Dragonfly Tramea Cophysa. *Ecotoxicology* **2021**, *30*, 1108–1115. [CrossRef]
12. Hashem, M.S.; Qi, X. Treated Wastewater Irrigation—A Review. *Water* **2021**, *13*, 1527. [CrossRef]
13. Tesfamariam, E.H.; Ogbazghi, Z.M.; Annandale, J.G.; Gebrehiwot, Y. Cost–Benefit Analysis of Municipal Sludge as a Low-Grade Nutrient Source: A Case Study from South Africa. *Sustainability* **2020**, *12*, 9950. [CrossRef]

14. Capodaglio, A.G.; Callegari, A. Feedstock and Process Influence on Biodiesel Produced from Waste Sewage Sludge. *J. Environ. Manag.* **2018**, *216*, 176–182. [CrossRef]
15. Ahmed, Y.; Zhong, J.; Yuan, Z.; Guo, J. Roles of Reactive Oxygen Species in Antibiotic Resistant Bacteria Inactivation and Micropollutant Degradation in Fenton and Photo-Fenton Processes. *J. Hazard. Mater.* **2022**, *430*, 128408. [CrossRef]
16. Madkhali, N.; Prasad, C.; Malkappa, K.; Choi, H.Y.; Govinda, V.; Bahadur, I.; Abumousa, R.A. Recent Update on Photocatalytic Degradation of Pollutants in Waste Water Using TiO_2-Based Heterostructured Materials. *Results Eng.* **2023**, *17*, 100920. [CrossRef]
17. Lazarotto, J.S.; de Lima Brombilla, V.; Silvestri, S.; Foletto, E.L. Conversion of Spent Coffee Grounds to Biochar as Promising TiO_2 Support for Effective Degradation of Diclofenac in Water. *Appl. Organomet. Chem.* **2020**, *34*, e6001. [CrossRef]
18. Peñas-Garzón, M.; Abdelraheem, W.H.M.; Belver, C.; Rodriguez, J.J.; Bedia, J.; Dionysiou, D.D. TiO_2-Carbon Microspheres as Photocatalysts for Effective Remediation of Pharmaceuticals under Simulated Solar Light. *Sep. Purif. Technol.* **2021**, *275*, 119169. [CrossRef]
19. Wang, J.; Wang, Y.; Wang, W.; Peng, T.; Liang, J.; Li, P.; Pan, D.; Fan, Q.; Wu, W. Visible Light Driven Ti^{3+} Self-Doped TiO_2 for Adsorption-Photocatalysis of Aqueous U(VI). *Environ. Pollut.* **2020**, *262*, 114373. [CrossRef] [PubMed]
20. Bi, Q.; Huang, X.; Dong, Y.; Huang, F. Conductive Black Titania Nanomaterials for Efficient Photocatalytic Degradation of Organic Pollutants. *Catal. Lett.* **2020**, *150*, 1346–1354. [CrossRef]
21. Nasr, M.; Eid, C.; Habchi, R.; Miele, P.; Bechelany, M. Recent Progress on Titanium Dioxide Nanomaterials for Photocatalytic Applications. *ChemSusChem* **2018**, *11*, 3023–3047. [CrossRef]
22. Chen, X.; Liu, L.; Yu, P.Y.; Mao, S.S. Increasing Solar Absorption for Photocatalysis with Black Hydrogenated Titanium Dioxide Nanocrystals. *Science* **2011**, *331*, 746–750. [CrossRef]
23. Zhu, G.; Xu, T.; Huang, F. The Black and White Issue of Nanotitania. In *Black TiO_2 Nanomaterials for Energy Applications*; World Scientific (Europe): London, UK, 2016; pp. 77–117. ISBN 978-1-78634-165-5.
24. Morgan, K.K. HIV Medications: Antiretroviral Therapy (ART)—Types, Brand Names, and How They Work. Available online: https://www.webmd.com/hiv-aids/aids-hiv-medication (accessed on 15 January 2025).
25. Ncube, S.; Madikizela, L.M.; Chimuka, L.; Nindi, M.M. Environmental Fate and Ecotoxicological Effects of Antiretrovirals: A Current Global Status and Future Perspectives. *Water Res.* **2018**, *145*, 231–247. [CrossRef] [PubMed]
26. Ngumba, E.; Gachanja, A.; Tuhkanen, T. Occurrence of Selected Antibiotics and Antiretroviral Drugs in Nairobi River Basin, Kenya. *Sci. Total Environ.* **2016**, *539*, 206–213. [CrossRef]
27. Castellino, S.; Moss, L.; Wagner, D.; Borland, J.; Song, I.; Chen, S.; Lou, Y.; Min, S.S.; Goljer, I.; Culp, A.; et al. Metabolism, Excretion, and Mass Balance of the HIV-1 Integrase Inhibitor Dolutegravir in Humans. *Antimicrob. Agents Chemother.* **2013**, *57*, 3536–3546. [CrossRef]
28. Jain, S.; Kumar, P.; Vyas, R.K.; Pandit, P.; Dalai, A.K. Occurrence and Removal of Antiviral Drugs in Environment: A Review. *Water. Air Soil Pollut.* **2013**, *224*, 1410. [CrossRef]
29. Madikizela, L.M.; Ncube, S.; Chimuka, L. Analysis, Occurrence and Removal of Pharmaceuticals in African Water Resources: A Current Status. *J. Environ. Manag.* **2020**, *253*, 109741. [CrossRef] [PubMed]
30. Ofrydopoulou, A.; Nannou, C.; Evgenidou, E.; Lambropoulou, D. Sample Preparation Optimization by Central Composite Design for Multi Class Determination of 172 Emerging Contaminants in Wastewaters and Tap Water Using Liquid Chromatography High-Resolution Mass Spectrometry. *J. Chromatogr. A* **2021**, *1652*, 462369. [CrossRef]
31. K'oreje, K.O.; Vergeynst, L.; Ombaka, D.; De Wispelaere, P.; Okoth, M.; Van Langenhove, H.; Demeestere, K. Occurrence Patterns of Pharmaceutical Residues in Wastewater, Surface Water and Groundwater of Nairobi and Kisumu City, Kenya. *Chemosphere* **2016**, *149*, 238–244. [CrossRef] [PubMed]
32. Madikizela, L.M.; Tavengwa, N.T.; Chimuka, L. Status of Pharmaceuticals in African Water Bodies: Occurrence, Removal and Analytical Methods. *J. Environ. Manag.* **2017**, *193*, 211–220. [CrossRef]
33. Reddy, K.; Renuka, N.; Kumari, S.; Bux, F. Algae-Mediated Processes for the Treatment of Antiretroviral Drugs in Wastewater: Prospects and Challenges. *Chemosphere* **2021**, *280*, 130674. [CrossRef]
34. Kebede, T.G.; Seroto, M.B.; Chokwe, R.C.; Dube, S.; Nindi, M.M. Adsorption of Antiretroviral (ARVs) and Related Drugs from Environmental Wastewaters Using Nanofibers. *J. Environ. Chem. Eng.* **2020**, *8*, 104049. [CrossRef]
35. Nannou, C.; Ofrydopoulou, A.; Evgenidou, E.; Heath, D.; Heath, E.; Lambropoulou, D. Antiviral Drugs in Aquatic Environment and Wastewater Treatment Plants: A Review on Occurrence, Fate, Removal and Ecotoxicity. *Sci. Total Environ.* **2020**, *699*, 134322. [CrossRef] [PubMed]
36. Kasprzyk-Hordern, B.; Dinsdale, R.M.; Guwy, A.J. Multiresidue Methods for the Analysis of Pharmaceuticals, Personal Care Products and Illicit Drugs in Surface Water and Wastewater by Solid-Phase Extraction and Ultra Performance Liquid Chromatography-Electrospray Tandem Mass Spectrometry. *Anal. Bioanal. Chem.* **2008**, *391*, 1293–1308. [CrossRef] [PubMed]
37. Horn, S.; Vogt, T.; Gerber, E.; Vogt, B.; Bouwman, H.; Pieters, R. HIV-Antiretrovirals in River Water from Gauteng, South Africa: Mixed Messages of Wastewater Inflows as Source. *Sci. Total Environ.* **2022**, *806*, 150346. [CrossRef]

38. Ngwenya, P.; Musee, N. Modelling Ecological Risks of Antiretroviral Drugs in the Environment. *Environ. Chem. Ecotoxicol.* **2023**, *5*, 145–154. [CrossRef]
39. Keller, V.D.J.; Williams, R.J.; Lofthouse, C.; Johnson, A.C. Worldwide Estimation of River Concentrations of Any Chemical Originating from Sewage-Treatment Plants Using Dilution Factors. *Environ. Toxicol. Chem.* **2014**, *33*, 447–452. [CrossRef] [PubMed]
40. Mtolo, S.P.; Mahlambi, P.N.; Madikizela, L.M. Synthesis and Application of a Molecularly Imprinted Polymer in Selective Solid-Phase Extraction of Efavirenz from Water. *Water Sci. Technol. J. Int. Assoc. Water Pollut. Res.* **2019**, *79*, 356–365. [CrossRef]
41. K'oreje, K.O.; Okoth, M.; Van Langenhove, H.; Demeestere, K. Occurrence and Treatment of Contaminants of Emerging Concern in the African Aquatic Environment: Literature Review and a Look Ahead. *J. Environ. Manag.* **2020**, *254*, 109752. [CrossRef]
42. Rimayi, C.; Odusanya, D.; Weiss, J.M.; De Boer, J.; Chimuka, L. Contaminants of Emerging Concern in the Hartbeespoort Dam Catchment and the uMngeni River Estuary 2016 Pollution Incident, South Africa. *Sci. Total Environ.* **2018**, *627*, 1008–1017. [CrossRef]
43. Wooding, M.; Rohwer, E.R.; Naudé, Y. Determination of Endocrine Disrupting Chemicals and Antiretroviral Compounds in Surface Water: A Disposable Sorptive Sampler with Comprehensive Gas Chromatography—Time-of-Flight Mass Spectrometry and Large Volume Injection with Ultra-High Performance Liquid Chromatography–Tandem Mass Spectrometry. *J. Chromatogr. A* **2017**, *1496*, 122–132. [CrossRef]
44. Gani, K.M.; Hlongwa, N.; Abunama, T.; Kumari, S.; Bux, F. Emerging Contaminants in South African Water Environment—A Critical Review of Their Occurrence, Sources and Ecotoxicological Risks. *Chemosphere* **2021**, *269*, 128737. [CrossRef]
45. Mutua, G.K.; Kinyari, P.; Githuku, C.; Kironchi, G.; Kang'ethe, E.; Prain, G.; Njenga, M.; Karanja, N.N. Assessment of Environmental and Public Health Hazards in Wastewater Used for Urban Agriculture in Nairobi, Kenya. *Trop. Subtrop. Agroecosystems* **2010**, *12*, 85–97.
46. Roura, M.; Watson-Jones, D.; Kahawita, T.M.; Ferguson, L.; Ross, D.A. Provider-Initiated Testing and Counselling Programmes in Sub-Saharan Africa: A Systematic Review of Their Operational Implementation. *AIDS* **2013**, *27*, 617–626. [CrossRef] [PubMed]
47. Semiyaga, S.; Okure, M.A.E.; Niwagaba, C.B.; Katukiza, A.Y.; Kansiime, F. Decentralized Options for Faecal Sludge Management in Urban Slum Areas of Sub-Saharan Africa: A Review of Technologies, Practices and End-Uses. *Resour. Conserv. Recycl.* **2015**, *104*, 109–119. [CrossRef]
48. Hawkins, T. Understanding and Managing the Adverse Effects of Antiretroviral Therapy. *Antiviral Res.* **2010**, *85*, 201–209. [CrossRef]
49. Olabode, G.; Somerset, V. Advances in Chromatographic Determination of Selected Anti-Retrovirals in Wastewater. In *Nano and Bio-Based Technologies for Wastewater Treatment*; Fosso-Kankeu, E., Ed.; Wiley: Hoboken, NJ, USA, 2019; pp. 105–127. ISBN 978-1-119-57709-6.
50. Almeida, L.C.; Mattos, A.C.; Dinamarco, C.P.G.; Figueiredo, N.G.; Bila, D.M. Chronic Toxicity and Environmental Risk Assessment of Antivirals in Ceriodaphnia Dubia and Raphidocelis Subcapitata. *Water Sci. Technol.* **2021**, *84*, 1623–1634. [CrossRef]
51. Robson, L.; Barnhoorn, I.E.J.; Wagenaar, G.M. The Potential Effects of Efavirenz on *Oreochromis mossambicus* after Acute Exposure. *Environ. Toxicol. Pharmacol.* **2017**, *56*, 225–232. [CrossRef]
52. Blas-García, A.; Apostolova, N.; Ballesteros, D.; Monleón, D.; Morales, J.M.; Rocha, M.; Victor, V.M.; Esplugues, J.V. Inhibition of Mitochondrial Function by Efavirenz Increases Lipid Content in Hepatic Cells. *Hepatology* **2010**, *52*, 115–125. [CrossRef] [PubMed]
53. Pitso, K.M. *Mozambique Tilapia Oreochromis mossambicus*; University of Johannesburg: Johannesburg, South Africa, 2020.
54. Omotola, E.O.; Genthe, B.; Ndlela, L.; Olatunji, O.S. Environmental Risk Characterization of an Antiretroviral (ARV) Lamivudine in Ecosystems. *Int. J. Environ. Res. Public Health* **2021**, *18*, 8358. [CrossRef]
55. Minguez, L.; Pedelucq, J.; Farcy, E.; Ballandonne, C.; Budzinski, H.; Halm-Lemeille, M.-P. Toxicities of 48 Pharmaceuticals and Their Freshwater and Marine Environmental Assessment in Northwestern France. *Environ. Sci. Pollut. Res.* **2016**, *23*, 4992–5001. [CrossRef]
56. Gosset, A.; Wiest, L.; Fildier, A.; Libert, C.; Giroud, B.; Hammada, M.; Hervé, M.; Sibeud, E.; Vulliet, E.; Polomé, P.; et al. Ecotoxicological Risk Assessment of Contaminants of Emerging Concern Identified by "Suspect Screening" from Urban Wastewater Treatment Plant Effluents at a Territorial Scale. *Sci. Total Environ.* **2021**, *778*, 146275. [CrossRef]
57. European Chemical Bureau. *Technical Guidance Document on Risk Assessment In-LBNC20418ENC.Pdf*; European Commission Joint Research Centre: Brussels, Belgium, 2003.
58. Musee, N.; Ondiaka, M.; Chimphango, A.; Aldrich, C. *Modelling the Fate, Behaviour and Toxicity of Engineered Nanomaterials in Aquatic Systems*; Water Research Commission: Pretoria, South Africa, 2015.
59. Hernando, M.D.; Mezcua, M.; Fernández-Alba, A.R.; Barceló, D. Environmental Risk Assessment of Pharmaceutical Residues in Wastewater Effluents, Surface Waters and Sediments. *Talanta* **2006**, *69*, 334–342. [CrossRef] [PubMed]
60. Kosma, C.I.; Lambropoulou, D.A.; Albanis, T.A. Investigation of PPCPs in Wastewater Treatment Plants in Greece: Occurrence, Removal and Environmental Risk Assessment. *Sci. Total Environ.* **2014**, *466–467*, 421–438. [CrossRef] [PubMed]
61. Molnar, E.; Maasz, G.; Pirger, Z. Environmental Risk Assessment of Pharmaceuticals at a Seasonal Holiday Destination in the Largest Freshwater Shallow Lake in Central Europe. *Environ. Sci. Pollut. Res.* **2021**, *28*, 59233–59243. [CrossRef]

62. Papageorgiou, M.; Kosma, C.; Lambropoulou, D. Seasonal Occurrence, Removal, Mass Loading and Environmental Risk Assessment of 55 Pharmaceuticals and Personal Care Products in a Municipal Wastewater Treatment Plant in Central Greece. *Sci. Total Environ.* **2016**, *543*, 547–569. [CrossRef] [PubMed]
63. Zhang, Y.; Zhang, T.; Guo, C.; Lv, J.; Hua, Z.; Hou, S.; Zhang, Y.; Meng, W.; Xu, J. Drugs of Abuse and Their Metabolites in the Urban Rivers of Beijing, China: Occurrence, Distribution, and Potential Environmental Risk. *Sci. Total Environ.* **2017**, *579*, 305–313. [CrossRef]
64. Muriuki, C.; Kairigo, P.; Home, P.; Ngumba, E.; Raude, J.; Gachanja, A.; Tuhkanen, T. Mass Loading, Distribution, and Removal of Antibiotics and Antiretroviral Drugs in Selected Wastewater Treatment Plants in Kenya. *Sci. Total Environ.* **2020**, *743*, 140655. [CrossRef]
65. Cid, R.S.; Roveri, V.; Vidal, D.G.; Dinis, M.A.P.; Cortez, F.S.; Salgueiro, F.R.; Toma, W.; Cesar, A.; Guimarães, L.L. Toxicity of Antiretrovirals on the Sea Urchin Echinometra Lucunter and Its Predicted Environmental Concentration in Seawater from Santos Bay (Brazilian Coastal Zone). *Resources* **2021**, *10*, 114. [CrossRef]
66. Guo, J.; Boxall, A.; Selby, K. Do Pharmaceuticals Pose a Threat to Primary Producers? *Crit. Rev. Environ. Sci. Technol.* **2015**, *45*, 2565–2610. [CrossRef]
67. Cayman Chemicals Safety Data Sheet. Available online: https://cdn.caymanchem.com/cdn/msds/14412m.pdf (accessed on 16 January 2025).
68. Vogt, B.; Bouwman, H.; Bezuidenhout, C.; Horn, S.; Bothma, L.; Gerber, E.; van Aswegen, D.; Blom, K.; Fouché, D.; Potgieter, J. *Quantification, Fate and Hazard Assessment of HIV-ARVs in Water Resources*; Water Research Commission: Pretoria, South Africa, 2020.
69. Kumar, A.; Raizada, P.; Hosseini-Bandegharaei, A.; Kumar Thakur, V.; Nguyen, V.-H.; Singh, P. C-, N-Vacancy Defect Engineered Polymeric Carbon Nitride towards Photocatalysis: Viewpoints and Challenges. *J. Mater. Chem. A* **2021**, *9*, 111–153. [CrossRef]
70. Liu, Y.; Yu, X.; Kamali, M.; Zhang, X.; Feijoo, S.; Al-Salem, S.M.; Dewil, R.; Appels, L. Biochar in Hydroxyl Radical-Based Electrochemical Advanced Oxidation Processes (eAOPs)—Mechanisms and Prospects. *Chem. Eng. J.* **2023**, *467*, 143291. [CrossRef]
71. Bermúdez, L.A.; Pascual, J.M.; Martínez, M.d.M.M.; Poyatos Capilla, J.M. Effectiveness of Advanced Oxidation Processes in Wastewater Treatment: State of the Art. *Water* **2021**, *13*, 2094. [CrossRef]
72. Cai, Q.Q.; Lee, B.C.Y.; Ong, S.L.; Hu, J.Y. Fluidized-Bed Fenton Technologies for Recalcitrant Industrial Wastewater Treatment–Recent Advances, Challenges and Perspective. *Water Res.* **2021**, *190*, 116692. [CrossRef] [PubMed]
73. Lebron, Y.A.R.; Moreira, V.R.; Maia, A.; Couto, C.F.; Moravia, W.G.; Amaral, M.C.S. Integrated Photo-Fenton and Membrane-Based Techniques for Textile Effluent Reclamation. *Sep. Purif. Technol.* **2021**, *272*, 118932. [CrossRef]
74. Rekhate, C.V.; Srivastava, J.K. Recent Advances in Ozone-Based Advanced Oxidation Processes for Treatment of Wastewater—A Review. *Chem. Eng. J. Adv.* **2020**, *3*, 100031. [CrossRef]
75. Reggiane de Carvalho Costa, L.; Guerra Pacheco Nunes, K.; Amaral Féris, L. Ultrasound as an Advanced Oxidative Process: A Review on Treating Pharmaceutical Compounds. *Chem. Eng. Technol.* **2021**, *44*, 1744–1758. [CrossRef]
76. Oluwole, A.O.; Omotola, E.O.; Olatunji, O.S. Pharmaceuticals and Personal Care Products in Water and Wastewater: A Review of Treatment Processes and Use of Photocatalyst Immobilized on Functionalized Carbon in AOP Degradation. *BMC Chem.* **2020**, *14*, 62. [CrossRef]
77. Friedmann, D. A General Overview of Heterogeneous Photocatalysis as a Remediation Technology for Wastewaters Containing Pharmaceutical Compounds. *Water* **2022**, *14*, 3588. [CrossRef]
78. Nabgan, W.; Saeed, M.; Jalil, A.A.; Nabgan, B.; Gambo, Y.; Ali, M.W.; Ikram, M.; Fauzi, A.A.; Owgi, A.H.K.; Hussain, I.; et al. A State of the Art Review on Electrochemical Technique for the Remediation of Pharmaceuticals Containing Wastewater. *Environ. Res.* **2022**, *210*, 112975. [CrossRef]
79. Finn, M.; Giampietro, G.; Mazyck, D.; Rodriguez, R. Activated Carbon for Pharmaceutical Removal at Point-of-Entry. *Processes* **2021**, *9*, 1091. [CrossRef]
80. Vinayagam, V.; Murugan, S.; Kumaresan, R.; Narayanan, M.; Sillanpää, M.; Viet N Vo, D.; Kushwaha, O.S.; Jenis, P.; Potdar, P.; Gadiya, S. Sustainable Adsorbents for the Removal of Pharmaceuticals from Wastewater: A Review. *Chemosphere* **2022**, *300*, 134597. [CrossRef]
81. Abujazar, M.S.S.; Karaağaç, S.U.; Abu Amr, S.S.; Alazaiza, M.Y.D.; Bashir, M.J.K. Recent Advancement in the Application of Hybrid Coagulants in Coagulation-Flocculation of Wastewater: A Review. *J. Clean. Prod.* **2022**, *345*, 131133. [CrossRef]
82. Ahmad, A.; Tariq, S.; Zaman, J.U.; Martin Perales, A.I.; Mubashir, M.; Luque, R. Recent Trends and Challenges with the Synthesis of Membranes: Industrial Opportunities towards Environmental Remediation. *Chemosphere* **2022**, *306*, 135634. [CrossRef]
83. Su, Z.; Wu, X.; Kuo, D.-H.; Yang, B.; Wu, B.; Chen, L.; Zhang, P.; Lin, J.; Lu, D.; Chen, X. Synergistic Vacancy Defects and Bandgap Engineering in an Ag/S Co-Doped Bi 2 O 3 -Based Sulfur Oxide Catalyst for Efficient Hydrogen Evolution. *J. Mater. Chem. A* **2024**, *12*, 10494–10506. [CrossRef]
84. Ahmed, S.; Rasul, M.G.; Martens, W.N.; Brown, R.; Hashib, M.A. Advances in Heterogeneous Photocatalytic Degradation of Phenols and Dyes in Wastewater: A Review. *Water. Air Soil Pollut.* **2011**, *215*, 3–29. [CrossRef]

85. Valencia, S.H.; Marín, J.M.; Restrepo, G.M. Evolution of Natural Organic Matter by Size Exclusion Chromatography during Photocatalytic Degradation by Solvothermal-Synthesized Titanium Dioxide. *J. Hazard. Mater.* **2012**, *213–214*, 318–324. [CrossRef] [PubMed]
86. Ibhadon, A.O.; Fitzpatrick, P. Heterogeneous Photocatalysis: Recent Advances and Applications. *Catalysts* **2013**, *3*, 189–218. [CrossRef]
87. Al-Rasheed, R.A. Water Treatment by Heterogeneous Photocatalysis an Overview. In Proceedings of the 4th SWCC Acquired Experience Symposium, Jeddah, Saudi Arabia, 7 May 2005.
88. Mohamadpour, F.; Amani, A. Mohammad Photocatalytic Systems: Reactions, Mechanism, and Applications. *RSC Adv.* **2024**, *14*, 20609–20645. [CrossRef]
89. Umar, M.; Aziz, H.A. Photocatalytic Degradation of Organic Pollutants in Water. In *Organic Pollutants—Monitoring, Risk and Treatment*; IntechOpen: London, UK, 2013; ISBN 978-953-51-0948-8.
90. Singh, S.; Garg, A. Characterisation and Utilization of Steel Industry Waste Sludge as Heterogeneous Catalyst for the Abatement of Chlorinated Organics by Advanced Oxidation Processes. *Chemosphere* **2020**, *242*, 125158. [CrossRef] [PubMed]
91. Gozdecka, A.; Wiącek, A.E. Effect of UV Radiation and Chitosan Coating on the Adsorption-Photocatalytic Activity of TiO_2 Particles. *Mater. Sci. Eng. C* **2018**, *93*, 582–594. [CrossRef]
92. Tehrani-Bagha, A.R.; Holmberg, K. Solubilization of Hydrophobic Dyes in Surfactant Solutions. *Materials* **2013**, *6*, 580–608. [CrossRef]
93. Marin, R.-C.; Behl, T.; Negrut, N.; Bungau, S. Management of Antiretroviral Therapy with Boosted Protease Inhibitors—Darunavir/Ritonavir or Darunavir/Cobicistat. *Biomedicines* **2021**, *9*, 313. [CrossRef] [PubMed]
94. Pascariu, P.; Cojocaru, C.; Samoila, P.; Airinei, A.; Olaru, N.; Rotaru, A.; Romanitan, C.; Tudoran, L.B.; Suchea, M. Cu/TiO_2 Composite Nanofibers with Improved Photocatalytic Performance under UV and UV–Visible Light Irradiation. *Surf. Interfaces* **2022**, *28*, 101644. [CrossRef]
95. Zhou, C.; Gao, J.; Deng, Y.; Wang, M.; Li, D.; Xia, C. Electric Double Layer-Mediated Polarization Field for Optimizing Photogenerated Carrier Dynamics and Thermodynamics. *Nat. Commun.* **2023**, *14*, 3592. [CrossRef]
96. Dugandžić, A.M.; Tomašević, A.V.; Radišić, M.M.; Šekuljica, N.Ž.; Mijin, D.Ž.; Petrović, S.D. Effect of Inorganic Ions, Photosensitisers and Scavengers on the Photocatalytic Degradation of Nicosulfuron. *J. Photochem. Photobiol. Chem.* **2017**, *336*, 146–155. [CrossRef]
97. Kumar, A.; Pandey, G. A Review on the Factors Affecting the Photocatalytic Degradation of Hazardous Materials. *Mater. Sci. Eng. Int. J.* **2017**, *1*, 106–114. [CrossRef]
98. Armaković, S.J.; Armaković, S.; Finčur, N.L.; Šibul, F.; Vione, D.; Šetrajčić, J.P.; Abramović, B.F. Influence of Electron Acceptors on the Kinetics of Metoprolol Photocatalytic Degradation in TiO_2 Suspension. A Combined Experimental and Theoretical Study. *RSC Adv.* **2015**, *5*, 54589–54604. [CrossRef]
99. Armaković, S.J.; Savanović, M.M.; Armaković, S. Titanium Dioxide as the Most Used Photocatalyst for Water Purification: An Overview. *Catalysts* **2023**, *13*, 26. [CrossRef]
100. Paumo, H.K.; Dalhatou, S.; Katata-Seru, L.M.; Kamdem, B.P.; Tijani, J.O.; Vishwanathan, V.; Kane, A.; Bahadur, I. TiO_2 Assisted Photocatalysts for Degradation of Emerging Organic Pollutants in Water and Wastewater. *J. Mol. Liq.* **2021**, *331*, 115458. [CrossRef]
101. Mahlambi, M.M.; Ngila, C.J.; Mamba, B.B. Recent Developments in Environmental Photocatalytic Degradation of Organic Pollutants: The Case of Titanium Dioxide Nanoparticles—A Review. *J. Nanomater.* **2015**, *2015*, 790173. [CrossRef]
102. Slusarski-Santana, V.; Fiorentin-Ferrari, L.D.; Fiorese, M.L. Antimicrobial Activities of Photocatalysts for Water Disinfection. In *Nanophotocatalysis and Environmental Applications: Detoxification and Disinfection*; Inamuddin Asiri, A.M., Lichtfouse, E., Eds.; Springer International Publishing: Cham, Switzerland, 2020; pp. 217–243. ISBN 978-3-030-12619-3.
103. Kapilashrami, M.; Zhang, Y.; Liu, Y.-S.; Hagfeldt, A.; Guo, J. Probing the Optical Property and Electronic Structure of TiO_2 Nanomaterials for Renewable Energy Applications. *Chem. Rev.* **2014**, *114*, 9662–9707. [CrossRef]
104. Basavarajappa, P.S.; Patil, S.B.; Ganganagappa, N.; Reddy, K.R.; Raghu, A.V.; Reddy, C.V. Recent Progress in Metal-Doped TiO_2, Non-Metal Doped/Codoped TiO_2 and TiO_2 Nanostructured Hybrids for Enhanced Photocatalysis. *Int. J. Hydrogen Energy* **2020**, *45*, 7764–7778. [CrossRef]
105. Aljaafari, A. Effect of Metal and Non-Metal Doping on the Photocatalytic Performance of Titanium Dioxide (TiO_2): A Review. *Curr. Nanosci.* **2022**, *18*, 499–519. [CrossRef]
106. Padmanabhan, N.T.; Thomas, N.; Louis, J.; Mathew, D.T.; Ganguly, P.; John, H.; Pillai, S.C. Graphene Coupled TiO_2 Photocatalysts for Environmental Applications: A Review. *Chemosphere* **2021**, *271*, 129506. [CrossRef]
107. Chauke, N.M.; Mohlala, R.L.; Ngqoloda, S.; Raphulu, M.C. Harnessing Visible Light: Enhancing TiO_2 Photocatalysis with Photosensitizers for Sustainable and Efficient Environmental Solutions. *Front. Chem. Eng.* **2024**, *6*, 1356021. [CrossRef]
108. Hassaan, M.A.; El-Nemr, M.A.; Elkatory, M.R.; Ragab, S.; Niculescu, V.-C.; El Nemr, A. Principles of Photocatalysts and Their Different Applications: A Review. *Top. Curr. Chem.* **2023**, *381*, 31. [CrossRef] [PubMed]

109. Ahmadpour, N.; Nowrouzi, M.; Madadi Avargani, V.; Sayadi, M.H.; Zendehboudi, S. Design and Optimization of TiO_2-Based Photocatalysts for Efficient Removal of Pharmaceutical Pollutants in Water: Recent Developments and Challenges. *J. Water Process Eng.* **2024**, *57*, 104597. [CrossRef]
110. Wu, S.; Hu, H.; Lin, Y.; Zhang, J.; Hu, Y.H. Visible Light Photocatalytic Degradation of Tetracycline over TiO_2. *Chem. Eng. J.* **2020**, *382*, 122842. [CrossRef]
111. Yang, H.; Li, G.; An, T.; Gao, Y.; Fu, J. Photocatalytic Degradation Kinetics and Mechanism of Environmental Pharmaceuticals in Aqueous Suspension of TiO_2: A Case of Sulfa Drugs. *Catal. Today* **2010**, *153*, 200–207. [CrossRef]
112. Chen, D.; Cheng, Y.; Zhou, N.; Chen, P.; Wang, Y.; Li, K.; Huo, S.; Cheng, P.; Peng, P.; Zhang, R.; et al. Photocatalytic Degradation of Organic Pollutants Using TiO_2-Based Photocatalysts: A Review. *J. Clean. Prod.* **2020**, *268*, 121725. [CrossRef]
113. Zou, L.; Zhu, Y.; Hu, Z.; Cao, X.; Cen, W. Remarkably Improved Photocatalytic Hydrogen Evolution Performance of Crystalline TiO_2 Nanobelts Hydrogenated at Atmospheric Pressure with the Assistance of Hydrogen Spillover. *Catal. Sci. Technol.* **2022**, *12*, 5575–5585. [CrossRef]
114. Qiang, C.; Li, N.; Zuo, S.; Guo, Z.; Zhan, W.; Li, Z.; Ma, J. Microwave-Assisted Synthesis of RuTe2/Black TiO_2 Photocatalyst for Enhanced Diclofenac Degradation: Performance, Mechanistic Investigation and Intermediates Analysis. *Sep. Purif. Technol.* **2022**, *283*, 120214. [CrossRef]
115. Zeng, Y.; Wang, Y.; Zhang, S.; Zhong, Q. A Study on the NH 3 -SCR Performance and Reaction Mechanism of a Cost-Effective and Environment-Friendly Black TiO_2 Catalyst. *Phys. Chem. Chem. Phys.* **2018**, *20*, 22744–22752. [CrossRef] [PubMed]
116. Andronic, L.; Ghica, D.; Stefan, M.; Mihalcea, C.G.; Vlaicu, A.-M.; Karazhanov, S. Visible-Light-Active Black TiO_2 Nanoparticles with Efficient Photocatalytic Performance for Degradation of Pharmaceuticals. *Nanomaterials* **2022**, *12*, 2563. [CrossRef] [PubMed]
117. Gad-Allah, T.A.; Ali, M.E.M.; Badawy, M.I. Photocatalytic Oxidation of Ciprofloxacin under Simulated Sunlight. *J. Hazard. Mater.* **2011**, *186*, 751–755. [CrossRef]
118. Padmapriya, G.; Manikandan, A.; Krishnasamy, V.; Jaganathan, S.K.; Antony, S.A. Spinel $NixZn_{1-x}Fe_2O_4$ ($0.0 \leq x \leq 1.0$) Nano-Photocatalysts: Synthesis, Characterization and Photocatalytic Degradation of Methylene Blue Dye. *J. Mol. Struct.* **2016**, *1119*, 39–47. [CrossRef]
119. El Bouraie, M.M.; Ibrahim, S.S. Comparative Study Between Metronidazole Residues Disposal by Using Adsorption and Photodegradation Processes onto MgO Nanoparticles. *J. Inorg. Organomet. Polym. Mater.* **2021**, *31*, 344–364. [CrossRef]
120. Wang, L.; Wang, Y.; Wang, Y.; Wang, H.; Wu, H.; Gao, D. Efficient Photocatalytic Degradation of Sulfonamides in Wastewater Using G-C_3N_4 Heterostructures: A Critical Review. *Environ. Technol. Innov.* **2024**, *36*, 103854. [CrossRef]
121. Nosaka, Y.; Nosaka, A. Understanding Hydroxyl Radical (•OH) Generation Processes in Photocatalysis. *ACS Energy Lett.* **2016**, *1*, 356–359. [CrossRef]
122. Tokode, O.; Prabhu, R.; Lawton, L.A.; Robertson, P.K.J. The Effect of pH on the Photonic Efficiency of the Destruction of Methyl Orange under Controlled Periodic Illumination with UV-LED Sources. *Chem. Eng. J.* **2014**, *246*, 337–342. [CrossRef]
123. Sarafraz, M.; Sadeghi, M.; Yazdanbakhsh, A.; Amini, M.M.; Sadani, M.; Eslami, A. Enhanced Photocatalytic Degradation of Ciprofloxacin by Black Ti^{3+}/N-TiO_2 under Visible LED Light Irradiation: Kinetic, Energy Consumption, Degradation Pathway, and Toxicity Assessment. *Process Saf. Environ. Prot.* **2020**, *137*, 261–272. [CrossRef]
124. Igwegbe, C.A.; Oba, S.N.; Aniagor, C.O.; Adeniyi, A.G.; Ighalo, J.O. Adsorption of Ciprofloxacin from Water: A Comprehensive Review. *J. Ind. Eng. Chem.* **2021**, *93*, 57–77. [CrossRef]
125. Abdullah, F.H.; Bakar, N.H.H.A.; Bakar, M.A. Current Advancements on the Fabrication, Modification, and Industrial Application of Zinc Oxide as Photocatalyst in the Removal of Organic and Inorganic Contaminants in Aquatic Systems. *J. Hazard. Mater.* **2022**, *424*, 127416. [CrossRef] [PubMed]
126. Tang, C.; Cheng, M.; Lai, C.; Li, L.; Yang, X.; Du, L.; Zhang, G.; Wang, G.; Yang, L. Recent Progress in the Applications of Non-Metal Modified Graphitic Carbon Nitride in Photocatalysis. *Coord. Chem. Rev.* **2023**, *474*, 214846. [CrossRef]
127. Ringu, T.; Ghosh, S.; Das, A.; Pramanik, N. Zinc Oxide Nanoparticles: An Excellent Biomaterial for Bioengineering Applications. *Emergent Mater.* **2022**, *5*, 1629–1648. [CrossRef]
128. Sun, C.; Xu, Q.; Xie, Y.; Ling, Y.; Hou, Y. Designed Synthesis of Anatase–TiO_2 (B) Biphase Nanowire/ZnO Nanoparticle Heterojunction for Enhanced Photocatalysis. *J. Mater. Chem. A* **2018**, *6*, 8289–8298. [CrossRef]
129. Ali, S.; Muhammad Ismail, P.; Khan, M.; Dang, A.; Ali, S.; Zada, A.; Raziq, F.; Khan, I.; Shakeel Khan, M.; Ateeq, M.; et al. Charge Transfer in TiO_2-Based Photocatalysis: Fundamental Mechanisms to Material Strategies. *Nanoscale* **2024**, *16*, 4352–4377. [CrossRef] [PubMed]
130. Qi, K.; Yu, J. Chapter 8—Modification of ZnO-Based Photocatalysts for Enhanced Photocatalytic Activity. In *Interface Science and Technology*; Yu, J., Jaroniec, M., Jiang, C., Eds.; Surface Science of Photocatalysis; Elsevier: Amsterdam, The Netherlands, 2020; Volume 31, pp. 265–284.
131. He, Y.; Sutton, N.B.; Rijnaarts, H.H.H.; Langenhoff, A.A.M. Degradation of Pharmaceuticals in Wastewater Using Immobilized TiO_2 Photocatalysis under Simulated Solar Irradiation. *Appl. Catal. B Environ.* **2016**, *182*, 132–141. [CrossRef]

132. Raliya, R.; Avery, C.; Chakrabarti, S.; Biswas, P. Photocatalytic Degradation of Methyl Orange Dye by Pristine Titanium Dioxide, Zinc Oxide, and Graphene Oxide Nanostructures and Their Composites under Visible Light Irradiation. *Appl. Nanosci.* **2017**, *7*, 253–259. [CrossRef]
133. Han, J.; Liu, Y.; Singhal, N.; Wang, L.; Gao, W. Comparative Photocatalytic Degradation of Estrone in Water by ZnO and TiO_2 under Artificial UVA and Solar Irradiation. *Chem. Eng. J.* **2012**, *213*, 150–162. [CrossRef]
134. Ravbar, M.; Kunčič, A.; Matoh, L.; Možina, S.S.; Šala, M.; Šuligoj, A. Controlled Growth of ZnO Nanoparticles Using Ethanolic Root Extract of Japanese Knotweed: Photocatalytic and Antimicrobial Properties. *RSC Adv.* **2022**, *12*, 31235–31245. [CrossRef]
135. Zhang, Z.; Zada, A.; Cui, N.; Liu, N.; Liu, M.; Yang, Y.; Jiang, D.; Jiang, J.; Liu, S. Synthesis of Ag Loaded ZnO/BiOCl with High Photocatalytic Performance for the Removal of Antibiotic Pollutants. *Crystals* **2021**, *11*, 981. [CrossRef]
136. Al-Ahmed, A. Photocatalytic Properties of Graphitic Carbon Nitrides (g-C_3N_4) for Sustainable Green Hydrogen Production: Recent Advancement. *Fuel* **2022**, *316*, 123381. [CrossRef]
137. Zhao, Z.; Ma, Y.; Fan, J.; Xue, Y.; Chang, H.; Masubuchi, Y.; Yin, S. Synthesis of Graphitic Carbon Nitride from Different Precursors by Fractional Thermal Polymerization Method and Their Visible Light Induced Photocatalytic Activities. *J. Alloys Compd.* **2018**, *735*, 1297–1305. [CrossRef]
138. Attri, P.; Garg, P.; Sharma, P.; Singh, R.; Chauhan, M.; Lim, D.-K.; Kumar, S.; Chaudhary, G.R. Precursor-Dependent Fabrication of Exfoliated Graphitic Carbon Nitride (gCN) for Enhanced Photocatalytic and Antimicrobial Activity under Visible Light Irradiation. *J. Clean. Prod.* **2023**, *422*, 138538. [CrossRef]
139. Nejad, M.S.; Vakily, Z.; Mostafavi, A.; Sheibani, H. Fabrication of Covalently Linked Ruthenium Complex onto Carbon Nitride Nanotubes for the Photocatalytic Degradation of Tetracycline Antibiotic. *preprint*, 2022. [CrossRef]
140. John, A.; Rajan, M.S.; Thomas, J. Carbon Nitride-Based Photocatalysts for the Mitigation of Water Pollution Engendered by Pharmaceutical Compounds. *Environ. Sci. Pollut. Res.* **2021**, *28*, 24992–25013. [CrossRef]
141. She, S.; Wang, Y.; Chen, R.; Yi, F.; Sun, C.; Hu, J.; Li, Z.; Lu, G.; Zhu, M. Ultrathin S-Doped Graphitic Carbon Nitride Nanosheets for Enhanced Sulpiride Degradation via Visible-Light-Assisted Peroxydisulfate Activation: Performance and Mechanism. *Chemosphere* **2021**, *266*, 128929. [CrossRef] [PubMed]
142. Hayat, A.; Al-Sehemi, A.G.; El-Nasser, K.S.; Taha, T.A.; Al-Ghamdi, A.A.; Syed, J.A.S.; Amin, M.A.; Ali, T.; Bashir, T.; Palamanit, A.; et al. Graphitic Carbon Nitride (g–C_3N_4)–Based Semiconductor as a Beneficial Candidate in Photocatalysis Diversity. *Int. J. Hydrogen Energy* **2022**, *47*, 5142–5191. [CrossRef]
143. Pazoki, M.; Parsa, M.; Farhadpour, R. Removal of the Hormones Dexamethasone (DXM) by Ag Doped on TiO_2 Photocatalysis. *J. Environ. Chem. Eng.* **2016**, *4*, 4426–4434. [CrossRef]
144. Evgenidou, E.; Vasilopoulou, K.; Ioannidou, E.; Koronaiou, L.A.; Nannou, C.; Trikkaliotis, D.G.; Bikiaris, D.; Kyzas, G.Z.; Lambropoulou, D. Photocatalytic Degradation of the Antiviral Drug Abacavir Using Titania-Graphene Oxide Nanocomposites in Landfill Leachate. *J. Photochem. Photobiol. Chem.* **2023**, *439*, 114628. [CrossRef]
145. Chen, J.; Luo, H.; Shi, H.; Li, G.; An, T. Anatase TiO_2 Nanoparticles–Carbon Nanotubes Composite: Optimization Synthesis and the Relationship of Photocatalytic Degradation Activity of Acyclovir in Water. *Appl. Catal. Gen.* **2014**, *485*, 188–195. [CrossRef]
146. Ayodhya, D. Ag-SPR and Semiconductor Interface Effect on a Ternary CuO@Ag@Bi_2S_3 Z-Scheme Catalyst for Enhanced Removal of HIV Drugs and (Photo)Catalytic Activity. *New J. Chem.* **2022**, *46*, 15838–15850. [CrossRef]
147. Bhembe, Y.A.; Lukhele, L.P.; Hlekelele, L.; Ray, S.S.; Sharma, A.; Vo, D.-V.N.; Dlamini, L.N. Photocatalytic Degradation of Nevirapine with a Heterostructure of Few-Layer Black Phosphorus Coupled with Niobium (V) Oxide Nanoflowers (FL-BP@Nb_2O_5). *Chemosphere* **2020**, *261*, 128159. [CrossRef]
148. Tabana, L.; Booysens, D.-R.; Tichapondwa, S. Photocatalytic Degradation of Efavirenz and Nevirapine Using Visible Light-Activated Ag-AgBr-LDH Nanocomposite Catalyst. *J. Photochem. Photobiol. Chem.* **2023**, *444*, 114997. [CrossRef]
149. An, T.; An, J.; Yang, H.; Li, G.; Feng, H.; Nie, X. Photocatalytic Degradation Kinetics and Mechanism of Antivirus Drug-Lamivudine in TiO_2 Dispersion. *J. Hazard. Mater.* **2011**, *197*, 229–236. [CrossRef]
150. Katal, R.; Davood Abadi Farahani, M.H.; Jiangyong, H. Degradation of Acetaminophen in a Photocatalytic (Batch and Continuous System) and Photoelectrocatalytic Process by Application of Faceted-TiO_2. *Sep. Purif. Technol.* **2020**, *230*, 115859. [CrossRef]
151. Feng, X.; Wang, P.; Hou, J.; Qian, J.; Wang, C.; Ao, Y. Oxygen Vacancies and Phosphorus Codoped Black Titania Coated Carbon Nanotube Composite Photocatalyst with Efficient Photocatalytic Performance for the Degradation of Acetaminophen under Visible Light Irradiation. *Chem. Eng. J.* **2018**, *352*, 947–956. [CrossRef]
152. Li, G.; Nie, X.; Gao, Y.; An, T. Can Environmental Pharmaceuticals Be Photocatalytically Degraded and Completely Mineralized in Water Using G-C_3N_4/TiO_2 under Visible Light Irradiation?—Implications of Persistent Toxic Intermediates. *Appl. Catal. B Environ.* **2016**, *180*, 726–732. [CrossRef]
153. Wu, M.; Lv, H.; Wang, T.; Ao, Z.; Sun, H.; Wang, C.; An, T.; Wang, S. Ag_2MoO_4 Nanoparticles Encapsulated in G-C_3N_4 for Sunlight Photodegradation of Pollutants. *Catal. Today* **2018**, *315*, 205–212. [CrossRef]
154. Hu, X.; Fan, J.; Zhang, K.; Yu, N.; Wang, J. Pharmaceuticals Removal by Novel Nanoscale Photocatalyst Bi_4VO_8Cl: Influencing Factors, Kinetics, and Mechanism. *Ind. Eng. Chem. Res.* **2014**, *53*, 14623–14632. [CrossRef]

155. Benjedim, S. *Preparation of Activated Carbons by Chemical Activation of Argan Seed Shell Waste. Application for the Removal of Paracetamol and Amoxicillin from Aqueous Solutions*; Universidad de Granada: Granada, Spain, 2022.
156. Kar, P.; Aggarwal, D.; Shukla, K.; Gupta, R.K. Defect State Modulation of TiO_2 Nanostructures for Photocatalytic Abatement of Emerging Pharmaceutical Pollutant in Wastewater Effluent. *Adv. Energy Sustain. Res.* **2022**, *3*, 2100162. [CrossRef]
157. Jin, D.; Lv, Y.; He, D.; Zhang, D.; Liu, Y.; Zhang, T.; Cheng, F.; Zhang, Y.; Sun, J.; Qu, J. Photocatalytic Degradation of COVID-19 Related Drug Arbidol Hydrochloride by Ti_3C_2 MXene/Supramolecular g-C_3N_4 Schottky Junction Photocatalyst. *Chemosphere* **2022**, *308*, 136461. [CrossRef] [PubMed]
158. Bhamare, V.S.; Kulkarni, R.M. Photocatalytic degradation of pharmaceutical drug zidovudine by undoped and 5% barium doped zinc oxide nanoparticles during water treatment: Synthesis and characterisation. *Int. J. Appl. Pharm.* **2019**, *11*, 227. [CrossRef]
159. Masunga, N.; Mamba, B.B.; Kefeni, K.K. Magnetically Separable Samarium Doped Copper Ferrite-Graphitic Carbon Nitride Nanocomposite for Photodegradation of Dyes and Pharmaceuticals under Visible Light Irradiation. *J. Water Process Eng.* **2022**, *48*, 102898. [CrossRef]
160. Fang, Y.; Li, Y.; Zhou, F.; Gu, P.; Liu, J.; Chen, D.; Li, N.; Xu, Q.; Lu, J. An Efficient Photocatalyst Based on Black TiO_2 Nanoparticles and Porous Carbon with High Surface Area: Degradation of Antibiotics and Organic Pollutants in Water. *ChemPlusChem* **2019**, *84*, 474–480. [CrossRef] [PubMed]
161. Zhu, C.; Chen, X.; Ma, J.; Gu, C.; Xian, Q.; Gong, T.; Sun, C. Carbon Nitride-Modified Defective TiO_{2-x}@Carbon Spheres for Photocatalytic H_2 Evolution and Pollutants Removal: Synergistic Effect and Mechanism Insight. *J. Phys. Chem. C* **2018**, *122*, 20444–20458. [CrossRef]
162. He, J.; Ye, J.; Zhang, Y.; Kong, L.; Zhou, X.; Ma, Y.; Yang, Y. Synergistic RGO/Black TiO_2/2D-ZIF-8 Ternary Heterogeneous Composite with Highly Efficient Photocatalytic Activity. *ChemistrySelect* **2020**, *5*, 3746–3755. [CrossRef]
163. Hojamberdiev, M.; Czech, B.; Wasilewska, A.; Boguszewska-Czubara, A.; Yubuta, K.; Wagata, H.; Daminova, S.S.; Kadirova, Z.C.; Vargas, R. Detoxifying SARS-CoV-2 Antiviral Drugs from Model and Real Wastewaters by Industrial Waste-Derived Multiphase Photocatalysts. *J. Hazard. Mater.* **2022**, *429*, 128300. [CrossRef]
164. Yuan, X.; Sun, M.; Yao, Y.; Lin, X.; Shi, J. N/Ti^{3+}-Codoped Triphasic TiO_2/g-C_3N_4 Heterojunctions as Visible-Light Photocatalysts for the Degradation of Organic Contaminants. *New J. Chem.* **2019**, *43*, 2665–2675. [CrossRef]
165. Wang, W.-L.; Wu, Q.-Y.; Wang, Z.-M.; Hu, H.-Y.; Negishi, N.; Torimura, M. Photocatalytic Degradation of the Antiviral Drug Tamiflu by UV-A/TiO_2: Kinetics and Mechanisms. *Chemosphere* **2015**, *131*, 41–47. [CrossRef]
166. Singh, J.; Palsaniya, S.; Soni, R.K. Mesoporous Dark Brown TiO_2 Spheres for Pollutant Removal and Energy Storage Applications. *Appl. Surf. Sci.* **2020**, *527*, 146796. [CrossRef]
167. Cao, S.; Du, M.; Li, Y.; Ye, X.; Wang, Y.; Ye, J. Nanosized Carbonate-Doped TiO_{2-x} Mesocrystals for Visible-Light-Driven Photocatalytic Removal of Water Pollutants. *ACS Appl. Nano Mater.* **2020**, *3*, 4197–4208. [CrossRef]
168. Wu, S.; Li, X.; Tian, Y.; Lin, Y.; Hu, Y.H. Excellent Photocatalytic Degradation of Tetracycline over Black Anatase-TiO_2 under Visible Light. *Chem. Eng. J.* **2021**, *406*, 126747. [CrossRef]
169. Alalm, M.G.; Djellabi, R.; Meroni, D.; Pirola, C.; Bianchi, C.L.; Boffito, D.C. Toward Scaling-Up Photocatalytic Process for Multiphase Environmental Applications. *Catalysts* **2021**, *11*, 562. [CrossRef]
170. Iervolino, G.; Zammit, I.; Vaiano, V.; Rizzo, L. Limitations and Prospects for Wastewater Treatment by UV and Visible-Light-Active Heterogeneous Photocatalysis: A Critical Review. In *Heterogeneous Photocatalysis: Recent Advances*; Muñoz-Batista, M.J., Navarrete Muñoz, A., Luque, R., Eds.; Springer International Publishing: Cham, Switzerland, 2020; pp. 225–264. ISBN 978-3-030-49492-6.
171. Constantino, D.S.M.; Dias, M.M.; Silva, A.M.T.; Faria, J.L.; Silva, C.G. Intensification Strategies for Improving the Performance of Photocatalytic Processes: A Review. *J. Clean. Prod.* **2022**, *340*, 130800. [CrossRef]
172. Beil, S.B.; Bonnet, S.; Casadevall, C.; Detz, R.J.; Eisenreich, F.; Glover, S.D.; Kerzig, C.; Næsborg, L.; Pullen, S.; Storch, G.; et al. Challenges and Future Perspectives in Photocatalysis: Conclusions from an Interdisciplinary Workshop. *JACS Au* **2024**, *4*, 2746–2766. [CrossRef]
173. Sibhatu, A.; Kassegn, G.; Imteyaz, S.; Suresh, S.; Tran, N.; Hessel, V. Synthesis and Process Parametric Effects on the Photocatalyst Efficiency of CuO Nanostructures for Decontamination of Toxic Heavy Metal Ions. *Chem. Eng. Process.—Process Intensif.* **2022**, *173*, 108814. [CrossRef]
174. Motamedi, M.; Yerushalmi, L.; Haghighat, F.; Chen, Z. Recent Developments in Photocatalysis of Industrial Effluents: A Review and Example of Phenolic Compounds Degradation. *Chemosphere* **2022**, *296*, 133688. [CrossRef]
175. Iqbal, M.A.; Akram, S.; khalid, S.; Lal, B.; Hassan, S.U.; Ashraf, R.; Kezembayeva, G.; Mushtaq, M.; Chinibayeva, N.; Hosseini-Bandegharaei, A. Advanced Photocatalysis as a Viable and Sustainable Wastewater Treatment Process: A Comprehensive Review. *Environ. Res.* **2024**, *253*, 118947. [CrossRef]
176. Raizada, P.; Sudhaik, A.; Singh, P. Photocatalytic Water Decontamination Using Graphene and ZnO Coupled Photocatalysts: A Review. *Mater. Sci. Energy Technol.* **2019**, *2*, 509–525. [CrossRef]
177. Kranz, C.; Wächtler, M. Characterizing Photocatalysts for Water Splitting: From Atoms to Bulk and from Slow to Ultrafast Processes. *Chem. Soc. Rev.* **2021**, *50*, 1407–1437. [CrossRef]

178. Zhang, W.; Li, G.; Liu, H.; Chen, J.; Ma, S.; Wen, M.; Kong, J.; An, T. Photocatalytic Degradation Mechanism of Gaseous Styrene over Au/TiO_2@CNTs: Relevance of Superficial State with Deactivation Mechanism. *Appl. Catal. B Environ.* **2020**, *272*, 118969. [CrossRef]
179. Bagheri, S.; TermehYousefi, A.; Do, T.-O. Photocatalytic Pathway toward Degradation of Environmental Pharmaceutical Pollutants: Structure, Kinetics and Mechanism Approach. *Catal. Sci. Technol.* **2017**, *7*, 4548–4569. [CrossRef]
180. Otor, H.O.; Steiner, J.B.; García-Sancho, C.; Alba-Rubio, A.C. Encapsulation Methods for Control of Catalyst Deactivation: A Review. *ACS Catal.* **2020**, *10*, 7630–7656. [CrossRef]
181. Zhang, Z.; He, D.; Zhao, S.; Qu, J. Recent Developments in Semiconductor-Based Photocatalytic Degradation of Antiviral Drug Pollutants. *Toxics* **2023**, *11*, 692. [CrossRef] [PubMed]